

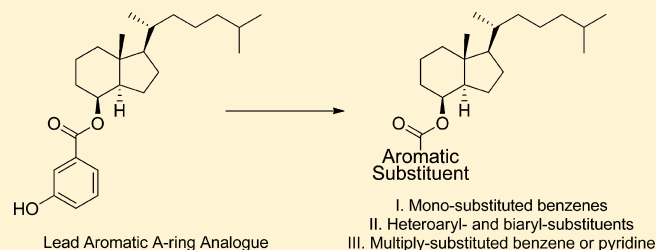
## Structure–Activity Relationships for Vitamin D3-Based Aromatic A-Ring Analogues as Hedgehog Pathway Inhibitors

Albert M. DeBerardinis, Daniel J. Madden, Upasana Banerjee, Vibhavari Sail, Daniel S. Raccuia, Daniel De Carlo, Steven M. Lemieux, Adam Meares, and M. Kyle Hadden\*

Department of Pharmaceutical Sciences, University of Connecticut, 69 North Eagleville Road, Unit 3092, Storrs, Connecticut 06269-3092, United States

### S Supporting Information

**ABSTRACT:** A structure–activity relationship study for a series of vitamin D3-based (VD3) analogues that incorporate aromatic A-ring mimics with varying functionality has provided key insight into scaffold features that result in potent, selective Hedgehog (Hh) pathway inhibition. Three analogue subclasses containing (1) a single substitution at the *ortho* or *para* position of the aromatic A-ring, (2) a heteroaryl or biaryl moiety, or (3) multiple substituents on the aromatic A-ring were prepared and evaluated. Aromatic A-ring mimics incorporating either single or multiple hydrophilic moieties on a six-membered ring inhibited the Hh pathway in both Hh-dependent mouse embryonic fibroblasts and cultured cancer cells (IC<sub>50</sub> values 0.74–10 μM). Preliminary studies were conducted to probe the cellular mechanisms through which VD3 and **5**, the most active analogue, inhibit Hh signaling. These studies suggested that the anti-Hh activity of VD3 is primarily attributed to the vitamin D receptor, whereas **5** affects Hh inhibition through a separate mechanism.

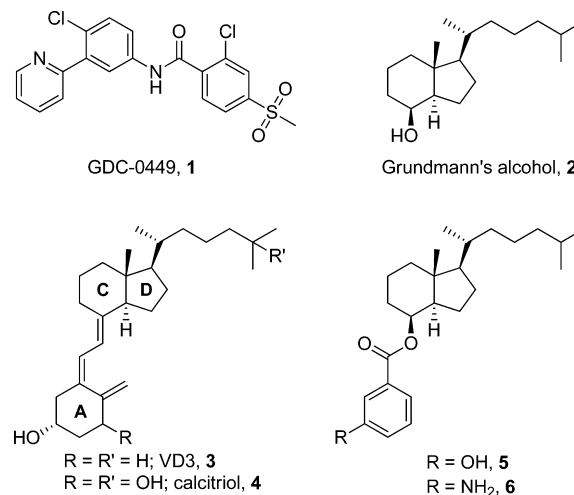


## INTRODUCTION

The Hedgehog (Hh) signaling pathway is a developmental pathway essential for directing normal growth and tissue patterning during embryonic development. Dysregulation of Hh signaling contributes to the onset and progression of several forms of human cancer, most notably basal cell carcinoma (BCC) and medulloblastoma (MB).<sup>1–3</sup> Both BCCs and MBs are widely recognized as Hh-dependent, and a significant number of BCCs (70%) and MBs (25%) exhibit detectable genetic mutations in Hh pathway components.<sup>4–6</sup> These mutations result in constitutive activation of the pathway and increased expression of Hh target genes, including several forms of the glioma-associated oncogene (Gli) family of signaling proteins.

Over the past decade, much attention across academia and industry has been targeted toward the identification of selective Hh signaling inhibitors as potential chemotherapeutic agents.<sup>7,8</sup> These studies have primarily focused on the development of synthetic small molecules as direct inhibitors of Smoothened (Smo), a GPCR-like 7-transmembrane protein that serves as a key regulator of Hh signaling and is the most druggable target in the pathway. The most advanced of these small molecules, GDC-0449 (Vismodegib, **1**, Chart 1), was approved by the FDA in early 2012 as the first-in-class Hh-specific antagonist for the treatment of locally advanced BCCs. While treatment of two MB patients with **1** also demonstrated initial positive results, relapse occurred when a point mutation in Smo (D473H) rendered the patient insensitive to further treatment with **1**.<sup>9,10</sup> In addition, a recent study reported that 21% of

### Chart 1. Hh Pathway Inhibitors



patients receiving continuous treatment of **1** for BCC developed regrowth of at least one BCC, suggesting resistance in BCC patients will also be an issue moving forward.<sup>11</sup> Finally, over half (54%) of basal cell nevus syndrome (BCNS) patients receiving **1** to treat BCCs voluntarily withdrew from the study due to adverse side effects.<sup>12</sup>

Received: November 22, 2013

Published: April 14, 2014

Table 1. Hh Inhibitory Activity for VD3 and Initial Analogues<sup>a</sup>

analogue	C3H10T1/2		ASZ		DAOY	
	Gli1 <sup>b</sup>	Cyp24A1 <sup>c</sup>	Gli1 <sup>b</sup>	Cyp24A1 <sup>c</sup>	Gli1 <sup>b</sup>	Cyp24A1 <sup>c</sup>
VD3	4.1 ± 0.3	8336 ± 38	2.1 ± 0.1	764 ± 24	>10	149 ± 90
2	3.1 ± 0.2	3.6 ± 0.5	>10	2.4 ± 0.9	>10	0.8 ± 0.1
5	0.74 ± 0.1	22.2 ± 4.7	5.2 ± 0.2	1.9 ± 0.1	3.7 ± 0.04	0.4 ± 0.1
6	2.8 ± 0.6	24.3 ± 3	7.1 ± 1	2.5 ± 1.4	9.2 ± 1.7	0.5 ± 0.1

<sup>a</sup>Data reproduced from refs 15 and 16. <sup>b</sup>IC<sub>50</sub> values (μM) represent the av ± SEM of at least two separate experiments performed in triplicate.

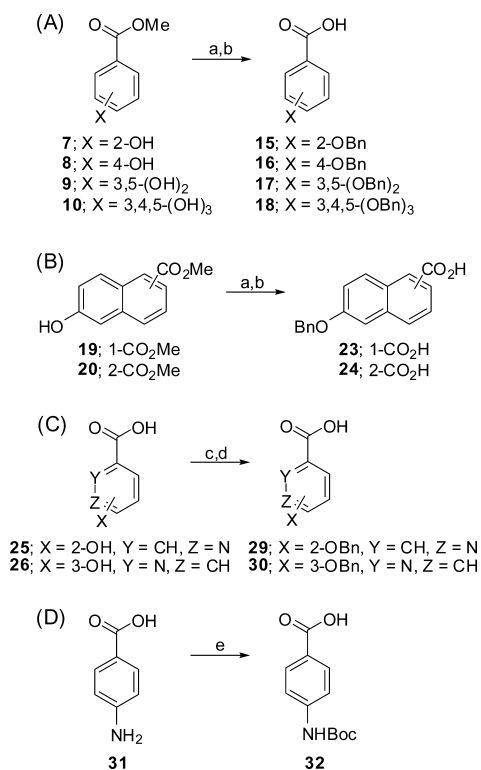
<sup>c</sup>Values represent Cyp24A1 mRNA expression relative to DMSO control (24 h, 5 μM).

Vitamin D3 (cholecalciferol, VD3, **3**) is a metabolic precursor to 1α,25-dihydroxyvitamin D3 (calcitriol, **4**), generally acknowledged as the hormonally active form of vitamin D. Both VD3 and calcitriol down-regulate Hh signaling in Hh-dependent cell culture and murine models of BCC; however, neither compound is a selective inhibitor of pathway signaling.<sup>13,14</sup> As calcitriol is known to exert a range of physiological effects via direct binding and activation of the nuclear vitamin D receptor (VDR), its nonselective nature is not surprising. By contrast, VD3 does not bind VDR and is commonly perceived to be physiologically inactive. This intriguing new activity for VD3 prompted a series of preliminary structure–activity relationship studies designed to identify the pharmacophore for VD3 inhibition of Hh signaling and serve as a starting point for developing selective inhibitors of Hh signaling based on the VD3 scaffold.<sup>15</sup> These initial studies identified Grundmann's alcohol (**2**) as comparable to VD3 in its ability to inhibit Hh signaling without activating canonical VDR signaling (Table 1). On the basis of these results, we designed, synthesized, and evaluated a small series of VD3 analogues in which the natural A-ring was replaced with an aromatic mimic.<sup>16</sup> Two compounds containing either a 3-phenol (**5**) or 3-aniline (**6**) linked to Grundmann's alcohol through an ester bond were identified as potent and selective inhibitors of pathway signaling in several Hh-dependent cell lines (Table 1). Further evaluation of analogues **2** and **5** demonstrated that the intact ester-linked scaffold was required for potent pathway inhibition, verifying this scaffold as an intriguing lead for further development. Herein, we report on an in-depth SAR study for this series of compounds and provide preliminary information as to the mechanistic aspects that govern its inhibition of Hh signaling.

## RESULTS AND DISCUSSION

**Chemistry.** We envisioned expanding the scope of the ester-linked series through the design and synthesis of a number of analogue subclasses based on modifications made to the aromatic motif. The ester linkage between Grundmann's alcohol and the aromatic A-ring mimics was maintained to explore this class of pathway inhibitors in an expeditious manner. Commercially available aromatic acids and esters were purchased and either coupled directly to **2** (acids) or coupled following standard protection/hydrolysis strategies shown in Scheme 1. For these studies, we prepared three series of analogues containing either (1) a single substitution at the *ortho* or *para* position of the aromatic A-ring, (2) a heteroaryl or biaryl moiety, or (3) multiple substituents on the aromatic A-ring.

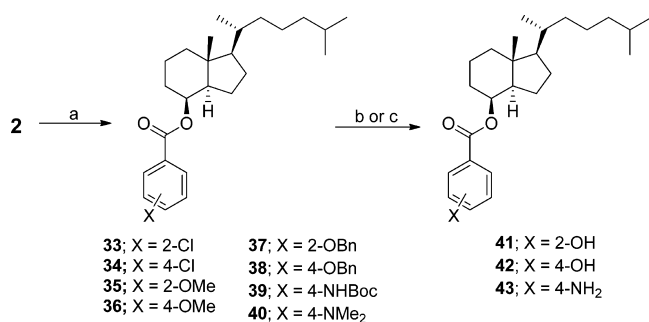
Benzyl bromide was utilized to protect the free phenols of methyl ester benzoates **7–10** and **19–20** as the benzyl ethers. Potassium or lithium hydroxide-mediated hydrolysis afforded carboxylic acids **15–18** and **23–24** in moderate to good yields

Scheme 1. Protection Schemes for Aromatic A-Ring Mimics<sup>a</sup>

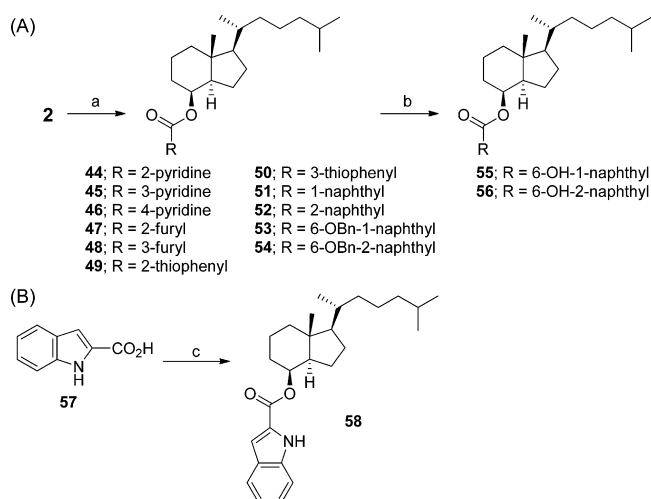
<sup>a</sup>Reagents and conditions: (a) BnBr, K<sub>2</sub>CO<sub>3</sub> (80–95%); (b) KOH or LiOH (50–80%); (c) BnBr, Cs<sub>2</sub>CO<sub>3</sub>, (50–65%); (d) 2 N NaOH (80%); (e) Boc<sub>2</sub>O, dioxane, 5% NaHCO<sub>3</sub> (70%).

(Scheme 1A,B). Similar protection of hydroxy-pyridine carboxylic acids **25–26** yielded both mono- and dibenzylated intermediates. The bis-protected compounds were readily separated via chromatography and sodium hydroxide-mediated hydrolysis afforded the carboxylic acids **29–30** (Scheme 1C). Finally, the aniline substituent of **31** was protected as the *t*-butoxycarbonyl using standard conditions (Scheme 1D). Standard esterification conditions (DCC and DMAP) were utilized to couple Grundmann's alcohol **2** to the requisite benzoic acid (Schemes 2 and 3A). Intermediates that required deprotection were submitted to the appropriate conditions and final analogues were isolated in good to excellent yields. Installing indole-2-carboxylic as the A-ring mimic was accomplished by preparing the acyl chloride in situ (oxalyl chloride and catalytic DMF), followed by coupling with **2** in the presence of DMAP (Scheme 3B).

**Biological Evaluation.** The initial evaluation of VD3 analogues as Hh pathway inhibitors was performed at a single dose (5 μM) by monitoring endogenous Gli1 mRNA levels in C3H10T1/2 cells, an Hh-dependent mouse embryonic

Scheme 2. Monosubstituted A-Ring Analogues: Subclass I<sup>a</sup>

<sup>a</sup>Reagents and conditions: (a) DCC, DMAP, DCM, (X)-ArCO<sub>2</sub>H (60–95%); (b) 37 or 38, Pd(OH)<sub>2</sub> (10%), H<sub>2</sub>, MeOH:THF (2:1) (75%); (c) 39, TFA:DCM (1:1) (65%).

Scheme 3. Hetero- and Biaryl A-Ring Analogues: Subclass II<sup>a</sup>

<sup>a</sup>Reagents and conditions: (a) DCC, DMAP, DCM, Aryl-CO<sub>2</sub>H, (60–95%); (b) 53 or 54, Pd(OH)<sub>2</sub> (10%), H<sub>2</sub>, MeOH:THF (2:1), (75%); (c) (i) oxalyl chloride, DMF, DCM, (ii) 2, DMAP, DCM (45%).

fibroblast (MEF). In addition, we have previously established that C3H10T1/2 cells respond to VDR activation with robust up-regulation of Cyp24A1, a well-characterized target gene of canonical vitamin D signaling; therefore, this assay provides a dual function for the determination of potency (Gli1 mRNA expression) and selectivity (Cyp24a1 mRNA expression) for VD3 analogues.<sup>13</sup> The protocol utilized for this assay was described previously,<sup>15,16</sup> and oxysterol activators of Hh signaling (OHCs; 20 $\alpha$ -hydroxycholesterol and 22(S)-hydroxycholesterol, 5  $\mu$ M each) were utilized to up-regulate Gli1 expression. Gli1 and Cyp24a1 mRNA expression levels were monitored following concomitant analogue and OHC addition. Results are provided in Tables 2–4 according to the VD3 analogue subclass.

As described previously, the addition of an aromatic A-ring mimic into the VD3 scaffold significantly enhances the Hh inhibitory properties of this class of VD3 analogues when compared to VD3 and 2.<sup>16</sup> Our initial SAR for this class of compounds focused on the incorporation of a variety of functional groups in the 3-position and identified both 5 and 6 as potent inhibitors of Hh signaling in MEFs that show promising anti-Hh activity in two cultured cancer cell lines

Table 2. Hh Inhibition for Monosubstituted VD3 Analogues

analogue <sup>a</sup>	Gli1 mRNA (%) <sup>b</sup>	Cyp24A1 mRNA <sup>c</sup>
DMSO	1.0	1.0
OHCs	100	
VD3	35.7 $\pm$ 0.3	8336 $\pm$ 38
1 <sup>d</sup>	4.8 $\pm$ 0.2	1.0 $\pm$ 0.02
2	46.4 $\pm$ 3.5	3.6 $\pm$ 0.5
5	1.9 $\pm$ 0.5	22.2 $\pm$ 4.7
6	2.4 $\pm$ 0.5	24.3 $\pm$ 3.0
33	109 $\pm$ 3	0.9 $\pm$ 0.1
34	77.7 $\pm$ 5.7	0.8 $\pm$ 0.01
35	98.0 $\pm$ 14	0.9 $\pm$ 0.3
36	113 $\pm$ 17	0.9 $\pm$ 0.2
40	107 $\pm$ 11	1.4 $\pm$ 0.2
41	115 $\pm$ 6.0	1.2 $\pm$ 0.1
42	2.4 $\pm$ 0.5	18.8 $\pm$ 10
43	15.4 $\pm$ 1.1	140 $\pm$ 10

<sup>a</sup>All analogues evaluated at 5  $\mu$ M and 24 h. <sup>b</sup>Values represent % Gli1 mRNA expression relative to OHC control (set as 100%). <sup>c</sup>Values represent up-regulation of Cyp24A1 mRNA normalized to DMSO (set to 1.0). <sup>d</sup>Compound 1 was evaluated at 0.5  $\mu$ M.

(Table 1).<sup>16</sup> To more fully explore SAR for the aromatic A-ring substituent, we first evaluated a series of analogues that incorporated a single functional group at either the 2- or 4-position. Interestingly, while incorporation of the phenol in the 4-position resulted in an analogue (42) that maintained potent inhibition of Hh signaling, shifting the phenol to the 2-position (41) resulted in complete loss of activity. There are two possible explanations for this observed result. First, placing the hydroxyl in the *ortho*-position may simply prevent it from accessing key interaction(s) available to the 3- or 4-phenol due to increased distance or orientation. Second, it is possible that being *ortho* to the ester linker orients the phenol such that it can form an intramolecular hydrogen bond with the carbonyl of the ester bond, preventing it from interacting with the binding site. Incorporating an amine in the 4-position (43) resulted in an analogue with slight decrease in activity when compared to the 3-position amine (6) (Gli1 expression = 15.4% and 2.4%, respectively). Similar to the 3-substituted analogues, incorporating a chlorine (33–34) or masking the phenol as the methoxy (35–36) resulted in analogues that did not inhibit pathway signaling. In addition, masking the 4-amine as the dimethylated amine (40) completely abolished the inhibitory activity. Similar to the results previously identified for 5 and 6, analogues that decreased Gli1 expression also moderately up-regulated Cyp24A1 (42–43).

The hetero- and biaryl analogue subclass was designed to (1) study whether incorporating functionality within the aromatic ring results in enhanced Hh inhibitory activity and (2) to explore steric constraints associated within the aromatic A-ring binding pocket (Table 3). An interesting trend was observed for the analogues incorporating a pyridine ring as the aromatic substituent (44–46). Whereas the 2-phenol did not inhibit Hh signaling, the 2-pyridyl substitution (44) provided an analogue that retained modest inhibition (Gli1 expression = 14.1%). Shifting the nitrogen to the 3- or 4-position resulted in a concomitant decrease in activity against the Hh pathway. This result is the opposite of that seen above when the substituent was appended to the ring. Finally, each of the pyridyl-containing analogues modestly up-regulated Cyp24A1 (14–57-fold) when compared to the other analogues in this subclass.

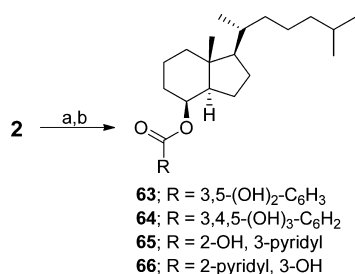
**Table 3. Hh Inhibition for Hetero- and Biaryl VD3 Analogues**

analogue <sup>a</sup>	Gli1 mRNA (%) <sup>b</sup>	Cyp24A1 mRNA <sup>c</sup>
44	14.1 ± 10	57.1 ± 10.3
45	20.7 ± 3.7	17.1 ± 1.4
46	51.1 ± 11	14.7 ± 6.7
47	95 ± 30	1.7 ± 0.5
48	91.5 ± 23	2.2 ± 1.3
49	109 ± 3	1.6 ± 0.4
50	109 ± 0.6	1.3 ± 0.6
51	82.3 ± 0.8	2.7 ± 1.0
52	77.4 ± 4	3.0 ± 0.2
55	103 ± 9	4.7 ± 4
56	91.9 ± 3	0.8 ± 0.1
58	84.5 ± 1.0	2.7 ± 0.3

<sup>a</sup>All analogues evaluated at 5  $\mu$ M and 24 h. <sup>b</sup>Values represent % Gli1 mRNA expression relative to OHC control (set as 100%). <sup>c</sup>Values represent up-regulation of Cyp24A1 mRNA normalized to DMSO (set to 1.0).

The five-membered heterocycles (47–50) did not inhibit Hh signaling nor did they activate VDR. Finally, the bicyclic aryl analogues (51–52, 55–56, 58) had no effects on Hh or VDR signaling. Taken together, these results indicate that a six-membered ring is the optimal size for the aromatic A-ring mimic.

The results for the first two subclasses of aromatic A-ring analogues suggest that potent Hh inhibition can be achieved by either incorporating a hydrogen bond donating substituent at the 3- or 4-position or utilizing a 2- or 3-pyridine moiety. On the basis of this SAR, a third class of analogues was designed to incorporate multiple substituents within the aromatic A-ring mimic to determine whether an additive effect could be achieved. These analogues contained either multiple hydroxyl groups (63–64) or a hydroxyl-substituted pyridine moiety (65–66) (Scheme 4). Interestingly, while the 3,5-dihydroxy

**Scheme 4. Aromatic A-Ring Analogues with Multiple Substitutions: Subclass III<sup>a</sup>**

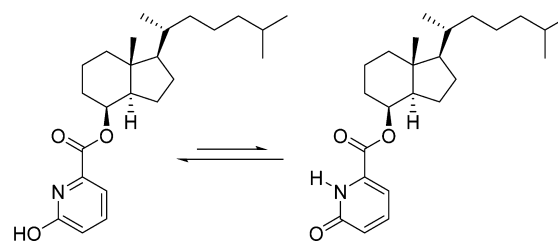
<sup>a</sup>Reagents and conditions: (a) DCC, DMAP, DCM, 17–18 or 29–30 (60–95%); (b) Pd(OH)<sub>2</sub> (10%), H<sub>2</sub>, MeOH:THF (2:1) (10–75%).

(63) and 3,4,5-trihydroxy (64) benzene derivatives demonstrated inhibition comparable to the singly substituted analogues, the hydroxyl-substituted pyridines (65–66) exhibited a significant decrease in activity (Table 4). It is possible that the decrease in potency demonstrated for these analogues is a result of isomerization in the aqueous environment between the pyridinol and a pyridinone moiety (Chart 2). This was observed in the benzylation of 26, where *N*-benzylation competes with phenolic-benzylation, as reported in the literature. Similar to the data for subclasses I and II, multiply

**Table 4. Hh Inhibition for Analogues with Multiple Substitutions**

analogue <sup>a</sup>	Gli1 mRNA (%) <sup>b</sup>	Cyp24A1 mRNA <sup>c</sup>
63	8.6 ± 2.2	19 ± 1
64	5.1 ± 1.3	11 ± 2
65	23.0 ± 1.0	7.5 ± 2
66	36.5 ± 3.6	3.1 ± 1

<sup>a</sup>All analogues evaluated at 5  $\mu$ M and 24 h. <sup>b</sup>Values represent % Gli1 mRNA expression relative to OHC control (set as 100%). <sup>c</sup>Values represent up-regulation of Cyp24A1 mRNA normalized to DMSO (set to 1.0).

**Chart 2. Potential Isomerization of Phenolic-Substituted Pyridine Analogue 66**

substituted analogues that retained Hh inhibition at this concentration (63–64) also demonstrated modest VDR activation (Cyp24A1 up-regulation = 11–19-fold).

Following the single concentration studies, we chose analogues from each subclass that demonstrated potent anti-Hh activity for concentration-dependent evaluation in C3H10T1/2, ASZ001 (murine BCC), and DAOY (human MB) cells. We also performed a more extensive analysis of VD3, 5, and 6 in these cellular models.<sup>16</sup> Both ASZ and DAOY cells have been utilized by our group and others as early stage models of Hh signaling in cultured cancer cells. For these studies, we chose to evaluate both Gli1 and Ptch expression to provide further support that down-regulation of Gli1 is related to Hh inhibition and not a result of other cellular mechanisms. Each analogue down-regulated Gli1 in a concentration-dependent fashion in C3H10T1/2 cells (Table 5). IC<sub>50</sub> values for these analogues (IC<sub>50</sub> range = 1.0–4.7  $\mu$ M) were comparable to those previously identified for 5 and 6. In addition, IC<sub>50</sub> values for down-regulation of Ptch in C3H10T1/2 cells closely followed those obtained for Gli1, highlighting the correlation between the two target genes in MEFs and providing strong support that this class of VD3 analogues is reducing Gli1 via inhibition of Hh signaling in this model.

The results of the concentration-dependent studies in cultured ASZ and DAOY cells provided an interesting contrast to the data from the MEFs. First, while the IC<sub>50</sub>s for down-regulation of Gli1 in ASZ for VD3 and the analogues (IC<sub>50</sub> range = 2.1–8.1  $\mu$ M) more closely mirrored those obtained in C3H10T1/2 cells, VD3 and several of the analogues had no effect on Gli1 expression in DAOY cells. In addition, there was decreased correlation between down-regulation of Gli1 and Ptch in both ASZ and DAOY cells. This may be the result of alterations within the gene encoding Ptch in these particular cancer cell lines. For example, loss of the wild-type *PTCH1* allele is characteristic of the ASZ line and drives Gli1 overexpression.<sup>14</sup> It is reasonable that Ptch1 mRNA modulation will not reflect an appropriate picture of Hh signaling and thus cannot be used to monitor Hh activity in these cells. Our previous analysis with known Hh signaling pathway inhibitors

Table 5. Concentration-Dependent Hh Inhibition for Representative VD3 Analogues

analogue	C3H10T1/2		ASZ		DAOY			VDR binding <sup>c</sup>
	Gli1 <sup>a</sup>	Ptch <sup>a</sup>	Gli1 <sup>a</sup>	Cyp24A1 <sup>b</sup>	Gli1 <sup>a</sup>	Ptch	Cyp24A1 <sup>b</sup>	
VD3	4.1 ± 0.3	2.9 ± 0.3	2.1 ± 0.1	764 ± 24	>10	>10	149 ± 90	>100
5	0.74 ± 0.1	1.1 ± 0.3	5.2 ± 0.2	1.9 ± 0.1	3.7 ± 0.04	3.6 ± 0.02	1.9 ± 0.9	>100
6	1.3 ± 0.3	2.5 ± 0.1	7.1 ± 1	2.5 ± 1.4	9.2 ± 1.7	>10	0.5 ± 0.1	>100
42	2.8 ± 0.6	3.3 ± 0.3	6.6 ± 0.7	6.3 ± 0.1	>10	>10	1.5 ± 0.4	>100
43	1.0 ± 0.04	2.9 ± 1.4	5.3 ± 0.4	2.1 ± 0.9	>10	>10	2.2 ± 1.4	>100
44	4.7 ± 1.3	12.6 ± 1.7	4.8 ± 1.2	4.8 ± 1.6	>10	>10	1.1 ± 0.2	>100
63	1.8 ± 0.6	4.5 ± 3.2	4.1 ± 0.4	3.6 ± 0.3	5.7 ± 0.9	>10	0.3 ± 0.01	>100
64	1.1 ± 0.1	1.3 ± 0.03	8.1 ± 0.2	1.3 ± 0.5	9.2 ± 1.7	>10	1.0 ± 0.3	>100

<sup>a</sup>IC<sub>50</sub> values (μM) represent the Mean ± SEM of at least two separate experiments performed in triplicate. <sup>b</sup>Values represent Cyp24A1 mRNA expression relative to DMSO control (24 h, 5 μM). <sup>c</sup>Values represent binding affinity for VD3 and VD3 analogues from at least two separate experiments. Calcitriol (4) is used as a positive control for VDR binding.

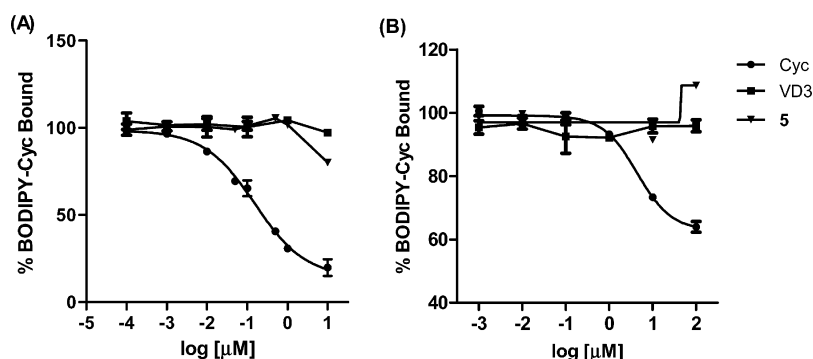


Figure 1. Displacement of BODIPY-Cyc by VD3 and 5 in HEK293T cells overexpressing Smo in intact cells (A) and isolated membranes (B). Data are from a representative experiment performed in triplicate.

(cyclopamine and 1) indicated that Gli1 down-regulation in ASZ cells correlates well with their reported activities in the standard Hh-dependent assay in MEFs;<sup>16</sup> however, measurement of Ptch1 expression failed to demonstrate significant down-regulation even at high concentrations of 1, VD3, or analogue (10 μM, data not shown). Similar observations were made in the DAOY cells, with only analogue 5 demonstrating Ptch1 down-regulation which correlated to the Gli1 data. As noted above with the ASZ cells, mutations within *PTCH1* have been implicated in MB formation and this may explain these inconsistencies across cell lines. Not surprisingly, none of the analogues significantly induced up-regulation of Cyp24A1 in either cancer cell line. Finally, the ability of these analogues to bind VDR was also analyzed in a fluorescence polarization-based competition assay.<sup>13,15,16</sup> We have demonstrated that neither VD3 nor any of the analogues tested displace the tight-binding fluorescent VDR ligand from full length human VDR in this assay at concentrations up to 100 μM, suggesting a lack of affinity for VDR (4 was used as a positive control in these experiments).

The only reported studies designed to characterize the mechanism through which VD3 inhibits Hh signaling have focused on the ability of cyclopamine (Cyc) to displace tritiated VD3 from an inducible form of human Smo in cultured yeast.<sup>17</sup> In an attempt to adapt a similar assay to a cultured mammalian cell system and to more fully explore the ability of VD3 and its analogues to bind Smo, we evaluated the ability of VD3 and 5 to displace BODIPY-Cyc from HEK293T cells overexpressing full length human Smo. Initially, we utilized flow cytometry to evaluate BODIPY-Cyc bound to intact cells. While nonlabeled Cyc displaced BODIPY-Cyc in a concentration-dependent

fashion, neither VD3 nor 5 demonstrated the ability to affect Cyc-Smo binding interactions up to 10 μM (Figure 1A). As these results were in direct contrast to those previously reported and to verify that these results were not assay specific, we also performed a fluorescence polarization assay with membranes isolated from the same Smo overexpressing HEK293T cells (Figure 1B). The results from this assay were similar to those observed with the intact cells, i.e., neither VD3 nor 5 displaced BODIPY-Cyc at concentrations up to 10 μM. In addition, we performed combination studies to determine whether VD3 or 5 could potentially synergize with GDC-0449 to enhance anti-Hh activity (Supporting Information Figure 1). Treatment with a single concentration of GDC-0449 (100 or 25 nM) did not result in a significant change in the IC<sub>50</sub> value of either VD3 or 5; however, GDC-0449 did enhance the overall efficacy of both VD3 and 5, suggesting the potential for additive effects. Similar results were demonstrated for the ability of VD3 (5 μM) or 5 (1 μM) to affect the Hh inhibitory activity of GDC-0449. While these results do not preclude the binding of VD3 or 5 to Smo as the means through which they regulate Hh signaling, they do suggest that neither compound binds in the Cyc/GDC-0449 binding site.

As noted above, several of the VD3 analogues identified as inhibitors of Hh signaling (5, 6, 43, and 44) also demonstrated modest activation of VDR, as measured by Cyp24A1 up-regulation (22–140-fold induction). Taken with our data demonstrating that VD3 and its analogues do not bind to the Cyc binding site on Smo, we sought to explore whether the anti-Hh activity for VD3 and this class of analogues is a downstream effect of VDR activation. For this study, we knocked down VDR expression in C3H10T1/2 cells with

VDR-specific siRNA to probe whether decreased expression of VDR affected the overall Hh inhibitory activity for VD3, calcitriol, and 5. Overall, treatment of C3H10T1/2 cells with VDR-specific siRNA significantly reduced VDR expression and did not affect Gli1 expression (Figure 2). Throughout our

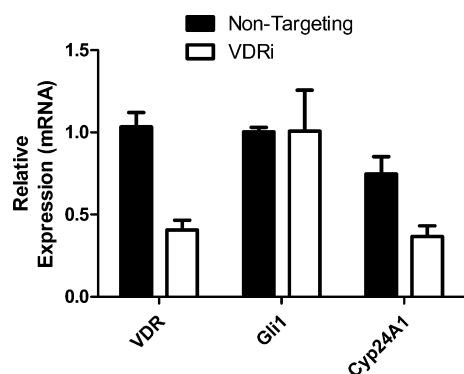


**Figure 2.** Expression of VDR, Gli1, and Cyp24A1 (mRNA) following nontargeting (filled) or VDR-specific (unfilled) RNAi transfection. Multiple experiments (>5) were performed, and data shown are from a representative experiment performed in triplicate.

experiments, treatment with VDRi resulted in consistent knockdown of VDR mRNA expression to 30–45% of nontargeting controls. Not surprisingly, the decrease in VDR expression resulted in a concomitant decrease in Cyp24A1 expression.

Once a suitable protocol was in place to reproducibly knockdown VDR in C3H10T1/2 cells, we evaluated the effects of Hh activation (OHCs) or inhibition (OHC + VD3, OHC + calcitriol, or OHC + 5) on VDR, Gli1, and Cyp24A1 expression (Figure 3). Neither activation of the Hh pathway nor pathway inhibition with 5 had an effect on VDR expression (Figure 3A); however, treatment with VD3 and calcitriol resulted in modest up-regulation of VDR expression in cells treated with both nontargeting and VDR-specific siRNA. VDR knockdown had no effect on the ability of OHCs to activate Hh signaling; however, concomitant treatment with either VD3, calcitriol, or 5 demonstrated interesting results. Knockdown of VDR completely abolished the ability of VD3 to decrease Gli1 expression and inhibit Hh signaling (Figure 3B). VD3 maintained its ability to significantly decrease Gli1 expression in cells treated with nontargeting siRNA, indicating the loss of Hh inhibition for VD3 is not a general result of the transfection protocol. By contrast, reduced VDR expression had no effect on the ability of either calcitriol or analogue 5 to inhibit Hh signaling. Finally, the reduced expression of VDR did not affect the ability of VD3 or calcitriol to significantly up-regulate Cyp24A1; however, the modest up-regulation of Cyp24A1 by 5 in nontargeting treated cells was completely abrogated in the presence of VDRi.

## DISCUSSION AND CONCLUSIONS

The initial identification of 5 as a potent, selective inhibitor of Hh signaling ( $IC_{50} = 0.74 \pm 0.1$ ) prompted the synthesis and evaluation of a series of related analogues to identify structure–activity relationships for this class of Hh pathway inhibitor. The preparation of this class of VD3 analogues was performed in an expeditious manner by linking aromatic functionalities designed to mimic the A-ring of VD3 to Grundmann's alcohol via an ester bond. Overall, SAR for this class of compounds

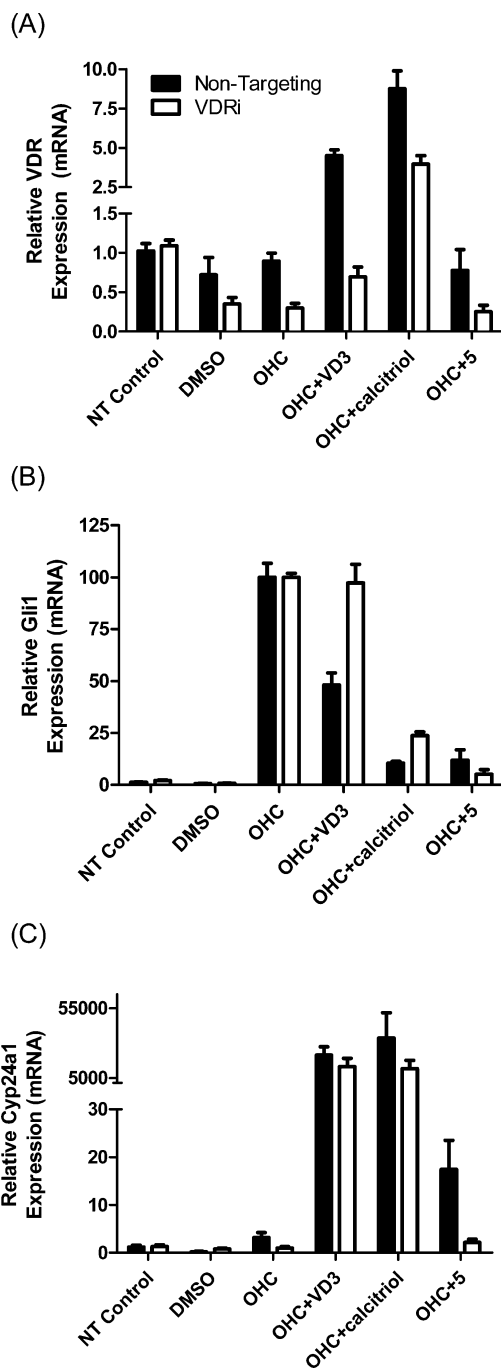


**Figure 3.** Effect of VDR expression level on Hh inhibition and VDR activation for VD3, 5, and calcitriol in C3H10T1/2 cells. Relative expression of VDR (A), Gli1 (B), and Cyp24A1 (C) in response to nontargeting (filled) and VDR-specific (open) RNAi transfection.

demonstrated that incorporation of a hydrophilic moiety in either the 3- or 4-position of the aromatic ring resulted in enhanced Hh inhibition and increased selectivity. Incorporating five-membered or biaryl aromatic moieties significantly reduced activity, suggesting that the six-membered phenyl ring is the optimal size for the aromatic A-ring mimic. Finally, the addition of multiple hydrophilic residues resulted in analogues that retained potent pathway inhibition; however, no additive effects were seen for analogues with multiple substituents. Concentration-dependent analysis of several analogues in Hh-dependent cancer cell lines further demonstrated the ability of this

class of compounds to selectively inhibit Hh signaling in vitro. Future generations of VD3-based analogues will explore the role of the ester linkage, modify the side chain region and incorporate functionality in the C-ring of the trans-hydrindane core of Grundmann's alcohol; all modifications designed to develop a more complete understanding of SAR for Hh inhibition of the VD3 scaffold.

An ester linkage between the northern CD-ring region and the aromatic A-ring isostere was chosen for these VD3 analogues due to its ease of formation and because analogue generation could be performed rapidly based on the parallel coupling of **2** with a library of commercially available aromatic acids. Esters are commonly used as prodrugs to provide enhanced bioavailability for carboxylic acids; however, they are not generally utilized as tethers in small molecule drugs due to the abundance of esterases in the human body that can contribute to their rapid metabolism. More recently, studies have demonstrated that esterase activity can be both cell-type and organelle-specific, resulting in enhanced stability of the parent compound.<sup>34–37</sup> Data from our studies provides strong evidence that our ester-linked VD3 analogues are stable in cell culture and that their anti-Hh activity is dependent on the intact scaffold. The parent alcohol **2** is a modest inhibitor of Hh signaling in C3H10T1/2 cells and is comparable to VD3 (IC<sub>50</sub> values = 3.1 and 4.1  $\mu$ M, respectively). Analogue **5** is significantly more potent in this cell line with an IC<sub>50</sub> value of 0.74  $\mu$ M. In addition, alcohol **2** is inactive against Hh signaling at concentrations up to 10  $\mu$ M in ASZ and DAOY cell lines; however, analogue **5** demonstrates modest activity in these cells (IC<sub>50</sub> values = 5.2 and 3.7  $\mu$ M, respectively). Finally, if **2** were responsible for the activity of the ester-linked analogues (through hydrolysis of the ester bond in the parent scaffold), it would be reasonable to expect there would be no discernible SAR and that our compounds would all demonstrate anti-Hh activity comparable to **2**. In fact, we see clear SAR for each different substitution pattern. Taken together, these data indicate that the ester-linked analogues are significantly more potent than the parent alcohol in multiple cellular contexts, providing strong evidence that the intact scaffold and not Grundmann's alcohol is primarily responsible for the anti-Hh activity of the compounds.

Studies designed to explore the cellular mechanisms through which VD3 and **5** inhibit Hh signaling focused on the two cellular receptors previously associated with VD3, VDR and Smo. As noted above, a tritiated analogue of VD3 was shown to selectively bind yeast cultures in which expression of human Smo had been chemically induced.<sup>17</sup> In addition, this binding was antagonized by the addition of Cyc. Results from our binding experiments suggest that neither VD3 nor **5** bind Smo in the Cyc binding pocket; however, this data does not preclude binding to another region of Smo. The recent identification of a second sterol binding site within the cysteine-rich domain (CRD) of Smo provides another region to explore for VD3/Smo binding interactions.<sup>38–40</sup> Preliminary analysis of VDR-mediated Hh inhibition for VD3 and **5** suggested that VDR is required for the anti-Hh effects of VD3 but not for calcitriol or analogue **5**. The inability of VD3 to maintain Hh inhibition in the presence of VDR knockdown was surprising for several reasons. First, similar studies performed in ASZ cells utilizing VDR-specific shRNA demonstrated that VDR knockdown did not affect the ability of VD3 to down-regulate Gli1 mRNA expression.<sup>11</sup> In addition, as demonstrated by our lab<sup>13</sup> and others,<sup>41</sup> calcitriol inhibits Hh signaling in vitro and in vivo and

these anti-Hh effects of calcitriol were not abrogated in *Vdr*<sup>-/-</sup> fibroblasts.<sup>41</sup> More specifically, the ability of calcitriol to inhibit Hh signaling in vitro has been localized to a step downstream of Ptch, suggesting its effects may also be mediated via Smo. As our assays (C3H10T1/2) and those previously reported (ASZ and fibroblasts) were performed in different cell lines, it is clear that cellular context is essential for determining the mechanisms through which VD3, calcitriol, and their analogues inhibit Hh signaling. In addition, the development of chemical probes that can definitively identify binding interactions between these *seco*-steroids and the Smo CRD will be necessary to further our understanding of whether the anti-Hh effects of these sterols are mediated via direct binding to Smo, or another, as yet unidentified, mechanism.

In conclusion, the synthesis and evaluation of a full series of aromatic A-ring VD3 analogues has provided insight into the structural requirements necessary for their potent, selective inhibition of Hh signaling. Ongoing SAR studies for this class of pathway inhibitors include modification to the ester linker as well as the aliphatic side chain. The results from these studies will provide a more comprehensive image of structural modalities that enhance pathway inhibition for the VD3 scaffold.

## ■ EXPERIMENTAL SECTION

**Chemical Synthesis. General Information.** VD3 used for chemical synthesis was purchased from HBCChem, Inc. Methyl ester phenols were purchased from Sigma-Aldrich or Fisher Scientific. ACS or HPLC grade methanol, acetone, tetrahydrofuran, and anhydrous DMF were purchased from Fisher Scientific. Anhydrous DCM (low water, <50 ppm water) was purchased from BrandNu Laboratories, Inc. (J.T. Baker solvent). All reactions were run under an inert atmosphere. NMR data was collected on a Bruker AVANCE 500 or 300 MHz spectrometer and analysis performed using MestReNova. HRMS data was analyzed at the Mass Spectrometry Facility at the University of Connecticut. Infrared (IR) analysis was performed on a Shimadzu FTIR-8400S spectrophotometer and analyzed with IR Solution software. The purity of all final compounds was determined to be  $\geq 95\%$  by HPLC on an LC-6AD Shimadzu LC instrument, equipped with Prominence auto sampler (SIL-20AC), UV/vis detector (SPD-20A), and communications bus module (CBM-20A). Compound purity was measured on 10  $\mu$ L of sample (dissolved in MeOH at 5–10 mM) on a Phenomenex Luna C18(2) 100A column (250 mm  $\times$  4.60 mm, 5  $\mu$ m) with precolumn (guard). One of four isocratic methods were used depending on the analogue (method A, 100% MeOH, 1.0 mL/min; method B, 98% MeOH:2% H<sub>2</sub>O, 1.0 mL/min; method C, 90% MeOH:10% H<sub>2</sub>O, 1 mL/min; or method D, 90% MeOH:10% H<sub>2</sub>O, 1.5 mL/min). Eluent was continuously monitored (254 nm), and data analysis was performed with Shimadzu LC Solution software.

**General Procedure for Benzoylation of Phenolic Esters.** To a solution of methyl ester phenol (6 mmol) in acetone (30 mL) was added benzyl bromide (15 mmol) followed by potassium carbonate as an anhydrous powder (36 mmol). The reaction was stirred at room temperature until the starting phenol was consumed (by TLC, 12–18 h). When the reaction was complete, the mixture was filtered over a Celite pad, washed with EtOAc, and concentrated. The crude residue was purified by column chromatography (SiO<sub>2</sub>, 5% EtOAc in hexanes) to afford the benzyl-protected phenols as a pale-yellow or clear oil (**11–12**) or off-white solid (**13–14**, **23–24**) in good yields (70–95%). Characterization of intermediates **11–14** and **22** was consistent with that previously reported.<sup>18–22</sup>

**Methyl 6-(benzyloxy)-1-naphthoate (21).** <sup>1</sup>H NMR (500 MHz, CDCl<sub>3</sub>)  $\delta$  8.97 (d, *J* = 9.4 Hz, 1H), 7.99 (dd, *J* = 7.3, 1.3 Hz, 1H), 7.80 (dd, *J* = 8.3 Hz, 1H), 7.38 (m, 2H), 7.35 (m, 1H), 7.30 (m, 2H), 7.23 (m, 2H), 7.17 (m, 1H), 5.10 (m, 2H). <sup>13</sup>C NMR (126 MHz CDCl<sub>3</sub>)  $\delta$  169.9, 156.4, 136.4, 135.1, 132.0, 128.4, 128.1, 127.8, 127.4, 127.3,

127.1, 126.8, 124.9, 120.2, 107.6, 69.8. DART-HRMS:  $m/z$  calcd for  $C_{25}H_{38}ClO_2NH_3$   $[MNH_4]^+$ , 422.2826; found, 422.2803.

**General Procedure for Benzoylation of (Hydroxy)pyridine Carboxylic Acids.** To a solution of carboxylic acid (10 mmol) in anhydrous DMF (30 mL) was added benzyl bromide (15 mmol) and cesium carbonate (60 mmol). The solution was stirred for 24 h at RT and diluted with water (100 mL) and EtOAc (100 mL). The organic layer was washed sequentially with saturated sodium bicarbonate (100 mL), water, 10% citric acid (100 mL), and saturated sodium chloride (100 mL). The EtOAc was dried ( $Na_2SO_4$ ), filtered, concentrated, and purified by column chromatography ( $SiO_2$ , 1–5% MeOH in DCM) to yield the benzylated methyl esters as either a yellow or white solid in moderate yield (65–70%). Characterization of intermediates 27–28 was consistent with that previously reported.<sup>23,24</sup>

**4-((tert-Butoxycarbonyl)amino)benzoic Acid (32).** 4-Aminobenzoic acid (1.5 g, 11 mmol) was dissolved in degassed (Ar-purged) 1,4-dioxane (20 mL) and 5% sodium bicarbonate (25 mL). The solution was cooled to 0 °C. While stirring vigorously, a solution of di-*tert*-butyl dicarbonate (3.6 g, 16.5 mmol) in degassed (Ar-purged) 1,4-dioxane (10 mL) was added dropwise. Following complete addition, the reaction was allowed to warm to RT and stirred for an additional 24 h. The solution was concentrated, redissolved in water (50 mL), and acidified to pH ~ 2 with dropwise addition of 3 N HCl. The aqueous layer was washed with EtOAc (2 × 100 mL), the combined organics were dried ( $Na_2SO_4$ ), filtered, and concentrated. The crude residue was purified by crystallization (EtOAc) and rinsed with cold EtOAc and copious amounts of hexanes to provide 32 as an off-white solid in good yield (70%).<sup>25</sup>

**General Procedure for Saponification of Methyl or Benzyl Esters.** To a stirred solution of ester (5 mmol) in THF (20 mL) was added potassium or lithium hydroxide (20%, aq; 20 mL). The solution was stirred at room temperature or refluxed for 12–24 h and adjusted to pH 7 with the dropwise addition of 3 N HCl upon completion of reaction. The pH of the solution was then brought to ~1–3 using 1 N HCl (note: in the case of substrates 65 and 66, pH was maintained at 7 for the extraction). The aqueous layer was washed with EtOAc (2 × 100 mL), and the combined organic layers were dried ( $Na_2SO_4$ ), filtered, and concentrated. The crude residue was purified by column chromatography ( $SiO_2$ , 30–50% EtOAc in hexanes) or crystallized from EtOAc to afford pure acids as white to off-white solids in good to excellent yield (45–90%). Characterization of intermediates 15–18 and 24 was consistent with that previously reported.<sup>22,26–29</sup>

**6-(Benzyloxy)-1-naphthoic Acid (23).** Yield 45%. <sup>1</sup>H NMR (500 MHz,  $CDCl_3$ :MeOD)  $\delta$  8.97 (d,  $J$  = 9.4 Hz, 1H), 7.99 (dd,  $J$  = 7.3, 1.3 Hz, 1H), 7.80 (dd,  $J$  = 8.3 Hz, 1H), 7.38 (m, 2H), 7.35 (m, 1H), 7.30 (m, 2H), 7.23 (m, 2H), 7.17 (m, 1H), 5.10 (m, 2H). <sup>13</sup>C NMR (126 MHz,  $CDCl_3$ :MeOD)  $\delta$  169.9, 156.4, 136.4, 135.1, 132.0, 128.4, 128.1, 127.8, 127.4, 127.3, 127.1, 126.8, 124.9, 120.2, 107.6, 69.8. DART-HRMS:  $m/z$  calcd for  $C_{25}H_{38}ClO_2NH_3$   $[MNH_4]^+$ , 422.2826; found, 422.2803.

**General Ester Coupling Protocol.** Grundmann's alcohol 2 (50 mg, 0.19 mmol), DCC (117 mg, 0.57 mmol), and DMAP (70 mg, 0.57 mmol) were dissolved in anhydrous DCM (4 mL) in an oven-dried round-bottom flask. Aromatic acid (0.57 mmol) was added and the solution stirred at RT for 12 h. The solvent was reduced to approximately 1.5 mL and the crude mixture purified with column chromatography ( $SiO_2$ , 4–60% EtOAc in hexanes) to yield coupled products as clear oils in moderate to good yields (30–95%).

**2-Chloro-VD3 Ester (33).** HPLC: >98%,  $R_t$  = 16.0 min (method D). <sup>1</sup>H NMR (500 MHz,  $CDCl_3$ )  $\delta$  7.79 (m, 1H), 7.45 (m, 1H), 7.40 (m, 1H), 7.31 (m, 1H), 5.44 (m, 1H), 2.04 (m, 2H), 1.81 (m, 2H), 1.52 (m, 5H), 1.34 (m, 3H), 1.24 (m, 2H), 1.12 (m, 4H), 1.00 (m, 1H), 0.92 (s, 3H), 0.90 (s, 3H), 0.87 (d,  $J$  = 2.2 Hz, 3H), 0.85 (d,  $J$  = 2.2 Hz, 3H). <sup>13</sup>C NMR (126 MHz  $CDCl_3$ )  $\delta$  165.5, 133.4, 132.0, 131.0, 130.9, 126.4, 73.0, 56.4, 51.4, 41.8, 39.9, 39.4, 35.9, 35.3, 30.5, 27.9, 27.0, 23.7, 22.7, 22.5, 18.5, 18.0, 13.2. IR (film)  $\nu_{max}$  2949, 2938, 2866, 1730, 1470, 1434, 1294, 1266, 1250, 1135, 1116, 1048, 937, 918, 746. DART-HRMS:  $m/z$  calcd for  $C_{25}H_{38}ClO_2NH_3$   $[MNH_4]^+$ , 422.2826; found, 422.2805.

**4-Chloro-VD3 Ester (34).** HPLC: 98%,  $R_t$  = 14.8 min (method B). <sup>1</sup>H NMR (500 MHz,  $CDCl_3$ )  $\delta$  7.98 (d,  $J$  = 8.6 Hz, 2H), 7.41 (d,  $J$  = 8.5 Hz, 2H), 5.39 (m, 1H), 2.07 (m, 1H), 1.98 (m, 1H), 1.82 (m, 2H), 1.54 (m, 6H), 1.38 (m, 4H), 1.24 (m, 3H), 1.13 (m, 4H), 1.01 (s, 3H), 0.93 (d,  $J$  = 6.5 Hz, 3H), 0.87 (d,  $J$  = 2.0 Hz, 3H), 0.86 (d,  $J$  = 2.0 Hz, 3H). <sup>13</sup>C NMR (126 MHz  $CDCl_3$ )  $\delta$  166.6, 139.0, 130.9, 129.3, 128.6, 72.6, 56.4, 51.5, 41.9, 39.8, 39.4, 35.9, 35.4, 30.5, 28.0, 27.0, 23.7, 22.8, 22.6, 22.5, 18.6, 18.0, 13.5. IR (film)  $\nu_{max}$  2949, 2930, 2866, 1720, 1716, 1286, 1266, 1256, 1113, 1102, 1092, 1015, 752. DART-HRMS:  $m/z$  calcd for  $C_{25}H_{38}ClO_2NH_3$   $[MNH_4]^+$ , 422.2826; found, 422.2803.

**2-Methoxy-VD3 Ester (35).** HPLC: 95%,  $R_t$  = 8.7 min (method B). <sup>1</sup>H NMR (500 MHz,  $CDCl_3$ )  $\delta$  7.81 (m, 1H), 7.46 (m, 1H), 6.97 (m, 2H), 5.39 (m, 1H), 3.89 (s, 3H), 2.02 (m, 2H), 1.81 (m, 2H), 1.51 (m, 7H), 1.34 (m, 3H), 1.23 (m, 2H), 1.11 (m, 4H), 0.97 (s, 3H), 0.87 (d,  $J$  = 6.4 Hz, 3H), 0.87 (d,  $J$  = 2.2 Hz, 3H), 0.86 (d,  $J$  = 2.2 Hz, 3H). <sup>13</sup>C NMR (126 MHz  $CDCl_3$ )  $\delta$  166.0, 159.1, 133.1, 131.5, 120.8, 119.9, 111.8, 71.9, 56.5, 55.7, 51.5, 41.8, 40.1, 39.4, 35.9, 35.4, 30.6, 28.0, 27.1, 23.7, 22.8, 22.6, 22.5, 18.6, 18.1, 13.2. IR (film)  $\nu_{max}$  2948, 2932, 2866, 2852, 1723, 1699, 1599, 1490, 1465, 1435, 1301, 1250, 1162, 1129, 1071, 753. DART-HRMS:  $m/z$  calcd for  $C_{26}H_{41}O_3$   $[MH]^+$ , 401.3055; found, 401.3100.

**4-Methoxy-VD3 Ester (36).** HPLC: >98%,  $R_t$  = 10.7 min (method B). <sup>1</sup>H NMR (500 MHz,  $CDCl_3$ )  $\delta$  8.01 (d,  $J$  = 8.8 Hz, 2H), 6.93 (d,  $J$  = 8.8 Hz, 2H), 5.37 (m, 1H), 3.86 (s, 3H), 2.06 (m, 1H), 1.98 (m, 1H), 1.82 (m, 2H), 1.52 (m, 6H), 1.39 (m, 4H), 1.24 (m, 2H), 1.14 (m, 4H), 1.03 (s, 3H), 0.93 (d,  $J$  = 6.5 Hz, 3H), 0.87 (d,  $J$  = 2.0 Hz, 3H), 0.86 (d,  $J$  = 1.9 Hz, 3H). <sup>13</sup>C NMR (126 MHz  $CDCl_3$ )  $\delta$  166.2, 163.1, 131.5, 123.3, 113.5, 71.8, 56.4, 55.4, 51.6, 41.9, 39.9, 39.4, 35.9, 35.4, 30.6, 28.0, 27.1, 23.7, 22.8, 22.6, 22.5, 18.6, 18.0, 13.5. IR (film)  $\nu_{max}$  2948, 2931, 2866, 1709, 1606, 1511, 1271, 1252, 1166, 1160, 1109, 1100, 1032, 846, 769. DART-HRMS:  $m/z$  calcd for  $C_{26}H_{41}O_3$   $[MH]^+$ , 401.3055; found, 401.3101.

**2-Benzyloxy-VD3 Ester (37).** <sup>1</sup>H NMR (500 MHz,  $CDCl_3$ )  $\delta$  7.80 (m, 1H), 7.47 (m, 2H), 7.38 (m, 3H), 7.30 (m, 1H), 6.98 (m, 2H), 5.42 (m, 1H), 5.19 (s, 2H), 1.98 (m, 2H), 1.81 (m, 1H), 1.69 (m, 1H), 1.51 (m, 5H), 1.42 (m, 2H), 1.34 (m, 3H), 1.26 (s, 1H), 1.14 (m, 6H), 1.00 (m, 1H), 0.93 (s, 3H), 0.91 (d,  $J$  = 6.5 Hz, 3H), 0.87 (dd,  $J$  = 6.6, 2.2 Hz, 6H). <sup>13</sup>C NMR (126 MHz  $CDCl_3$ )  $\delta$  166.0, 157.9, 136.7, 132.8, 131.3, 128.5, 127.7, 127.0, 121.8, 120.3, 113.6, 71.9, 70.5, 56.4, 51.5, 41.8, 40.0, 39.4, 35.9, 35.3, 30.6, 27.9, 27.1, 23.7, 22.8, 22.7, 22.5, 18.6, 18.0, 13.3. DART-HRMS:  $m/z$  calcd for  $C_{32}H_{44}O_3$   $[MH]^+$ , 477.3369; found, 477.3421.

**4-Benzyloxy-VD3 Ester (38).** <sup>1</sup>H NMR (500 MHz,  $CDCl_3$ )  $\delta$  8.06 (d,  $J$  = 8.6 Hz, 2H), 7.46 (m, 4H), 7.37 (m, 1H), 7.04 (d,  $J$  = 8.6 Hz, 2H), 5.43 (m, 1H), 5.16 (s, 2H), 2.11 (m, 1H), 2.03 (m, 1H), 1.87 (m, 2H), 1.56 (m, 5H), 1.44 (m, 3H), 1.31 (m, 3H), 1.18 (m, 4H), 1.08 (s, 3H), 0.99 (d,  $J$  = 6.5 Hz, 3H), 0.92 (dd,  $J$  = 6.5, 1.9 Hz, 6H). <sup>13</sup>C NMR (126 MHz  $CDCl_3$ )  $\delta$  166.2, 162.3, 136.3, 131.5, 128.6, 128.1, 127.4, 123.6, 114.4, 71.9, 70.0, 56.5, 51.6, 41.9, 39.5, 35.9, 35.4, 30.6, 28.0, 27.1, 23.7, 22.8, 22.6, 22.5, 18.6, 18.0, 13.5. DART-HRMS:  $m/z$  calcd for  $C_{32}H_{44}O_3$   $[MH]^+$ , 477.3369; found, 477.3385.

**4-((tert-Butoxycarbonyl)amino)-VD3 Ester (39).** <sup>1</sup>H NMR (500 MHz,  $CDCl_3$ )  $\delta$  7.98 (m, 2H), 7.42 (m, 2H), 6.62 (br s, 1H), 5.37 (m, 1H), 2.06 (m, 1H), 1.97 (m, 1H), 1.81 (m, 2H), 1.54 (m, 6H), 1.53 (s, 9H), 1.42 (m, 2H), 1.33 (m, 3H), 1.23 (m, 3H), 1.13 (m, 4H), 1.01 (s, 3H), 0.93 (d,  $J$  = 6.5 Hz, 3H), 0.86 (m, 6H). <sup>13</sup>C NMR (126 MHz  $CDCl_3$ )  $\delta$  166.1, 152.1, 142.4, 130.8, 125.2, 117.3, 72.0, 69.4, 56.4, 51.6, 41.9, 39.9, 39.5, 35.9, 35.4, 30.6, 29.7, 28.2, 28.0, 27.0, 23.7, 22.8, 22.6, 22.5, 18.6, 18.0, 13.5. DART-HRMS:  $m/z$  calcd for  $C_{30}H_{47}NO_4$   $[M]^+$ , 485.3505; found, 485.3509.

**4-Dimethylamino-VD3 Ester (40).** Analogue 40 was afforded in 80% yield using the following alternate method: 4-Dimethylaminocarboxylic acid (1 mmol) was reacted with oxalyl chloride (2.6 mmol) in DCM (10 mL) at 0 °C with 2 drops of DMF for 2 h. The reaction was then stirred at room temperature for 16 h. The solvent was removed and the mixture redissolved in DCM (6 mL), and 2 (0.5 mmol) in DCM, 3 mL) was added dropwise at room temperature and stirred for 24 h. The reaction was quenched by addition of sodium bicarbonate (satd aq; 30 mL), washed with DCM (1 × 50 mL), and purified with column chromatography ( $SiO_2$ , 5% EtOAc in hexanes).

HPLC: 99%,  $R_t = 11.3$  min (method B).  $^1\text{H NMR}$  (500 MHz,  $\text{CDCl}_3$ )  $\delta$  7.93 (m, 2H), 6.66 (m, 2H), 5.37 (m, 1H), 3.03 (s, 6H), 2.06 (m, 1H), 1.98 (m, 1H), 1.81 (m, 2H), 1.51 (m, 5H), 1.34 (m, 3H), 1.24 (m, 3H), 1.12 (m, 4H), 1.04 (s, 3H), 1.00 (m, 1H), 0.93 (d,  $J = 6.5$  Hz, 3H), 0.88 (d,  $J = 2.0$  Hz, 3H), 0.87 (d,  $J = 2.0$  Hz, 3H).  $^{13}\text{C NMR}$  (126 MHz,  $\text{CDCl}_3$ )  $\delta$  166.8, 153.1, 131.1, 117.8, 110.7, 71.0, 56.5, 51.7, 41.9, 40.0, 39.4, 35.9, 35.3, 30.7, 29.6, 27.9, 27.1, 23.7, 22.7, 22.6, 22.5, 18.6, 18.0, 13.5. IR (film)  $\nu_{\text{max}}$  3011, 3002, 2940, 2933, 2924, 2911, 2903, 2890, 2866, 2854, 1694, 1606, 1526, 1467, 1445, 1366, 1343, 1317, 1285, 1273, 1233, 1216, 1183, 1159, 1109, 1063, 946, 829, 757, 667. DART-HRMS:  $m/z$  calcd for  $\text{C}_{27}\text{H}_{44}\text{NO}_2$   $[\text{MH}]^+$ , 414.3372; found, 414.3388.

**2-Pyridyl-VD3 Ester (44).** HPLC: >98%,  $R_t = 19.0$  min (method D).  $^1\text{H NMR}$  (500 MHz,  $\text{CDCl}_3$ )  $\delta$  8.76 (m, 1H), 8.04 (m, 1H), 7.80 (m, 1H), 7.43 (m, 1H), 5.47 (m, 1H), 2.04 (m, 2H), 1.82 (m, 2H), 1.52 (m, 5H), 1.40 (m, 2H), 1.31 (m, 2H), 1.22 (m, 2H), 1.11 (m, 4H), 1.02 (s, 3H), 0.91 (d,  $J = 6.6$  Hz, 3H), 0.85 (d,  $J = 1.8$  Hz, 3H), 0.84 (d,  $J = 1.9$  Hz, 3H).  $^{13}\text{C NMR}$  (126 MHz  $\text{CDCl}_3$ )  $\delta$  164.5, 150.1, 148.6, 136.8, 126.4, 124.6, 73.1, 56.3, 51.5, 41.8, 39.8, 39.4, 35.8, 35.3, 30.4, 27.9, 27.0, 23.7, 22.7, 22.6, 22.5, 18.5, 17.9, 13.4. IR (film)  $\nu_{\text{max}}$  3060, 2946, 2942, 2920, 2905, 2863, 1737, 1716, 1583, 1571, 1466, 1436, 1383, 1366, 1305, 1276, 1244, 1130, 1135, 1086, 1060, 1044, 993, 939, 918, 745, 704, 618. DART-HRMS:  $m/z$  calcd for  $\text{C}_{32}\text{H}_{44}\text{NO}_2$   $[\text{MH}]^+$ , 372.2903; found, 372.2889.

**3-Pyridyl-VD3 Ester (45).** HPLC: >98%,  $R_t = 25.0$  min (method D).  $^1\text{H NMR}$  (500 MHz,  $\text{CDCl}_3$ )  $\delta$  9.25 (br s, 1H), 8.78 (br s, 1H), 8.29 (m, 1H), 7.39 (m, 1H), 5.43 (m, 1H), 2.07 (m, 1H), 1.99 (m, 1H), 1.81 (m, 2H), 1.54 (m, 5H), 1.40 (m, 2H), 1.33 (m, 2H), 1.24 (m, 3H), 1.12 (m, 4H), 1.01 (s, 3H), 0.92 (d,  $J = 6.5$  Hz, 3H), 0.86 (d,  $J = 2.0$  Hz, 3H), 0.85 (d,  $J = 1.9$  Hz, 3H).  $^{13}\text{C NMR}$  (126 MHz  $\text{CDCl}_3$ )  $\delta$  165.1, 153.1, 150.8, 137.0, 126.7, 123.3, 73.0, 56.4, 51.4, 41.8, 39.7, 39.4, 35.8, 35.3, 30.5, 27.9, 27.0, 23.7, 22.7, 22.6, 22.5, 18.5, 17.9, 13.5. IR (film)  $\nu_{\text{max}}$  2929, 2921, 2907, 2896, 2867, 1723, 1717, 1590, 1467, 1418, 1362, 1325, 1287, 1274, 1266, 1235, 1122, 1117, 741, 702. DART-HRMS:  $m/z$  calcd for  $\text{C}_{32}\text{H}_{44}\text{NO}_2$   $[\text{MH}]^+$ , 372.2903; found, 372.2897.

**4-Pyridyl-VD3 Ester (46).** HPLC: >98%,  $R_t = 27.9$  min (method D).  $^1\text{H NMR}$  (500 MHz,  $\text{CDCl}_3$ )  $\delta$  8.77 (m, 2H), 7.84 (m, 2H), 5.42 (m, 1H), 2.07 (m, 1H), 1.98 (m, 1H), 1.81 (m, 2H), 1.53 (m, 5H), 1.36 (m, 4H), 1.23 (m, 3H), 1.12 (m, 4H), 1.01 (s, 3H), 0.92 (d,  $J = 6.5$  Hz, 3H), 0.86 (d,  $J = 2.0$  Hz, 3H), 0.85 (d,  $J = 1.9$  Hz, 3H).  $^{13}\text{C NMR}$  (126 MHz  $\text{CDCl}_3$ )  $\delta$  164.9, 150.5, 138.0, 122.8, 73.4, 56.3, 51.4, 41.8, 39.7, 39.4, 35.8, 35.3, 30.4, 27.9, 26.9, 23.7, 22.7, 22.6, 22.5, 18.5, 17.9, 13.5. IR (film)  $\nu_{\text{max}}$  2955, 2948, 2935, 2870, 2868, 1723, 1653, 1635, 1623, 1467, 1407, 1323, 1287, 1274, 1213, 1121, 1063, 938, 917, 849, 749, 707, 670. DART-HRMS:  $m/z$  calcd for  $\text{C}_{32}\text{H}_{44}\text{NO}_2$   $[\text{MH}]^+$ , 372.2903; found, 372.2892.

**2-Furyl-VD3 Ester (47).** HPLC: 99%,  $R_t = 7.5$  min (method B).  $^1\text{H NMR}$  (500 MHz,  $\text{CDCl}_3$ )  $\delta$  7.58 (m, 1H), 7.11 (m, 1H), 6.50 (m, 1H), 5.38 (m, 1H), 2.05 (m, 1H), 1.96 (m, 1H), 1.81 (m, 2H), 1.50 (m, 5H), 1.38 (m, 4H), 1.23 (m, 2H), 1.12 (m, 4H), 1.00 (m, 1H), 0.99 (s, 3H), 0.92 (d,  $J = 6.5$  Hz, 3H), 0.87 (d,  $J = 2.0$  Hz, 3H), 0.86 (d,  $J = 2.0$  Hz, 3H).  $^{13}\text{C NMR}$  (126 MHz,  $\text{CDCl}_3$ )  $\delta$  158.7, 146.2, 144.9, 117.2, 111.6, 72.2, 56.2, 51.3, 41.8, 39.7, 39.3, 35.8, 35.3, 30.4, 27.9, 27.0, 23.6, 22.8, 22.5, 18.5, 17.8, 13.1. IR (film)  $\nu_{\text{max}}$  3141, 3121, 2962, 2945, 2934, 2927, 2920, 2912, 2887, 2851, 2253, 1794, 1712, 1580, 1568, 1461, 1397, 1374, 1301, 1277, 1228, 1174, 1158, 1115, 1013, 981, 941, 915, 763, 733, 615, 596. DART-HRMS:  $m/z$  calcd for  $\text{C}_{23}\text{H}_{36}\text{O}_3\text{NH}_4$   $[\text{MNH}_4]^+$ , 378.3008; found, 378.2983.

**3-Furyl-VD3 Ester (48).** HPLC: >98%,  $R_t = 16.3$  min (method C).  $^1\text{H NMR}$  (500 MHz,  $\text{CDCl}_3$ )  $\delta$  7.98 (m, 1H), 7.41 (m, 1H), 6.74 (m, 1H), 5.33 (m, 1H), 2.04 (m, 1H), 1.95 (m, 1H), 1.79 (m, 2H), 1.50 (m, 5H), 1.37 (m, 3H), 1.22 (m, 2H), 1.12 (m, 4H), 1.00 (m, 1H), 0.97 (s, 3H), 0.92 (d,  $J = 6.4$  Hz, 3H), 0.87 (d,  $J = 2.0$  Hz, 3H), 0.86 (d,  $J = 2.0$  Hz, 3H).  $^{13}\text{C NMR}$  (126 MHz,  $\text{CDCl}_3$ )  $\delta$  162.8, 147.4, 143.5, 120.0, 109.8, 71.6, 56.5, 51.4, 41.8, 39.9, 39.4, 35.9, 35.3, 30.5, 27.9, 27.0, 23.7, 22.7, 22.6, 22.5, 18.5, 17.9, 13.2. IR (film)  $\nu_{\text{max}}$  2932, 2925, 2901, 2895, 2865, 2858, 2851, 1726, 1704, 1699, 1637, 1457,

1381, 1309, 1216, 1149, 1111, 1064, 1032, 985, 873, 760, 667. DART-HRMS:  $m/z$  calcd for  $\text{C}_{23}\text{H}_{36}\text{O}_3$   $[\text{M}]^+$ , 360.2664; found, 360.2668.

**2-Thiophenyl-VD3 Ester (49).** HPLC: >98%,  $R_t = 25.9$  min (method C).  $^1\text{H NMR}$  (500 MHz,  $\text{CDCl}_3$ )  $\delta$  7.79 (m, 1H), 7.53 (m, 1H), 7.10 (m, 1H), 5.35 (m, 1H), 2.06 (m, 1H), 1.98 (m, 1H), 1.81 (m, 2H), 1.52 (m, 5H), 1.41 (m, 2H), 1.33 (m, 2H), 1.12 (m, 4H), 1.02 (s, 3H), 0.93 (d,  $J = 6.5$  Hz, 3H), 0.87 (d,  $J = 2.0$  Hz, 3H), 0.86 (d,  $J = 2.0$  Hz, 3H).  $^{13}\text{C NMR}$  (126 MHz,  $\text{CDCl}_3$ )  $\delta$  162.0, 134.6, 133.0, 131.9, 127.6, 72.5, 56.4, 51.5, 41.8, 39.9, 39.4, 35.9, 35.3, 34.9, 30.5, 27.9, 27.0, 23.7, 22.7, 22.6, 22.5, 18.5, 17.9, 13.3. IR (film)  $\nu_{\text{max}}$  2939, 2925, 2908, 2895, 2866, 2855, 2118, 1703, 1700, 1525, 1467, 1444, 1418, 1382, 1366, 1357, 1286, 1257, 1231, 1224, 1160, 1090, 1075, 1034, 938, 917, 861, 750, 715. DART-HRMS:  $m/z$  calcd for  $\text{C}_{23}\text{H}_{36}\text{O}_2\text{SNH}_4$   $[\text{MNH}_4]^+$ , 394.2780; found, 394.2775.

**3-Thiophenyl-VD3 Ester (50).** HPLC: >99%,  $R_t = 39.6$  min (method C).  $^1\text{H NMR}$  (500 MHz,  $\text{CDCl}_3$ )  $\delta$  8.08 (m, 1H), 7.53 (m, 1H), 7.30 (m, 1H), 5.35 (m, 1H), 2.06 (m, 1H), 1.97 (m, 1H), 1.81 (m, 2H), 1.51 (m, 5H), 1.38 (m, 4H), 1.24 (m, 3H), 1.13 (m, 4H), 1.02 (s, 3H), 0.93 (d,  $J = 6.5$  Hz, 3H), 0.88 (d,  $J = 1.9$  Hz, 3H), 0.86 (d,  $J = 1.9$  Hz, 3H).  $^{13}\text{C NMR}$  (126 MHz,  $\text{CDCl}_3$ )  $\delta$  162.6, 134.5, 132.2, 127.9, 125.8, 71.9, 56.5, 51.5, 41.9, 39.9, 39.4, 35.9, 35.4, 30.5, 27.9, 27.0, 23.7, 22.7, 22.6, 22.5, 18.6, 18.0, 13.4. IR (film)  $\nu_{\text{max}}$  3146, 2977, 2947, 2929, 2924, 2896, 2863, 2856, 2845, 1722, 1704, 1523, 1519, 1463, 1444, 1408, 1382, 1374, 1261, 1253, 1203, 1187, 1159, 1100, 1060, 982, 943, 917, 873, 858, 841, 821, 747, 695. DART-HRMS:  $m/z$  calcd for  $\text{C}_{23}\text{H}_{36}\text{O}_2\text{SNH}_4$   $[\text{MNH}_4]^+$ , 394.2780; found, 394.2779.

**1-Naphthyl-VD3 Ester (51).** HPLC: 97%,  $R_t = 15.9$  min (method B).  $^1\text{H NMR}$  (500 MHz,  $\text{CDCl}_3$ )  $\delta$  8.99 (m, 1H), 8.19 (m, 1H), 8.01 (m, 1H), 7.88 (m, 1H), 7.62 (m, 1H), 7.52 (m, 2H), 5.54 (m, 1H), 2.09 (m, 2H), 1.86 (m, 2H), 1.57 (m, 6H), 1.36 (m, 3H), 1.27 (m, 2H), 1.15 (m, 4H), 1.03 (m, 1H), 1.01 (s, 3H), 0.94 (d,  $J = 6.5$  Hz, 3H), 0.89 (d,  $J = 2.1$  Hz, 3H), 0.88 (d,  $J = 2.3$  Hz, 3H).  $^{13}\text{C NMR}$  (126 MHz,  $\text{CDCl}_3$ )  $\delta$  167.2, 133.8, 132.9, 131.4, 129.6, 128.4, 127.9, 127.5, 126.1, 125.9, 124.4, 72.1, 56.5, 51.6, 41.9, 40.0, 39.4, 35.9, 35.4, 30.7, 28.0, 27.1, 23.7, 22.8, 22.8, 22.5, 18.6, 18.1, 13.4. IR (film)  $\nu_{\text{max}}$  3051, 2947, 2933, 2923, 2909, 2866, 2850, 1713, 1594, 1510, 1466, 1382, 1374, 1365, 1274, 1244, 1235, 1215, 1160, 1132, 1076, 1063, 1003, 937, 812, 782, 757, 508. DART-HRMS:  $m/z$  calcd for  $\text{C}_{29}\text{H}_{40}\text{O}_2$   $[\text{M}]^+$ , 420.3028; found, 420.3022.

**2-Naphthyl-VD3 Ester (52).** HPLC: 96%,  $R_t = 17.0$  min (method B).  $^1\text{H NMR}$  (500 MHz,  $\text{CDCl}_3$ )  $\delta$  8.62 (m, 1H), 8.09 (m, 1H), 7.96 (m, 1H), 7.88 (m, 2H), 7.56 (m, 2H), 5.49 (m, 1H), 2.09 (m, 2H), 1.89 (m, 2H), 1.57 (m, 6H), 1.44 (m, 1H), 1.36 (m, 2H), 1.27 (m, 3H), 1.16 (m, 3H), 1.13 (s, 3H), 0.96 (d,  $J = 6.5$  Hz, 3H), 0.89 (d,  $J = 1.9$  Hz, 3H), 0.88 (d,  $J = 1.9$  Hz, 3H).  $^{13}\text{C NMR}$  (126 MHz,  $\text{CDCl}_3$ )  $\delta$  166.6, 135.3, 132.4, 130.9, 129.3, 128.1, 128.0, 127.6, 126.5, 125.2, 72.3, 56.4, 51.6, 41.9, 39.9, 39.4, 35.9, 35.4, 30.6, 27.9, 27.0, 23.7, 22.7, 22.7, 22.5, 18.6, 18.0, 13.5. IR (film)  $\nu_{\text{max}}$  3058, 2986, 2965, 2898, 2855, 2849, 2843, 2116, 1722, 1705, 1629, 1601, 1463, 1456, 1383, 1373, 1365, 1352, 1289, 1254, 1206, 1185, 1159, 1130, 1091, 954, 918, 860, 778, 761, 473. DART-HRMS:  $m/z$  calcd for  $\text{C}_{29}\text{H}_{40}\text{O}_2$   $[\text{M}]^+$ , 420.3028; found, 420.3024.

**6-Benzyloxy-1-naphthyl-VD3 Ester (53).**  $^1\text{H NMR}$  (500 MHz,  $\text{CDCl}_3$ )  $\delta$  8.92 (m, 1H), 8.03 (m, 1H), 7.88 (m, 1H), 7.49 (m, 2H), 7.42 (m, 3H), 7.35 (2H), 7.25 (m, 2H), 5.51 (m, 1H), 5.21 (s, 2H), 2.07 (m, 1H), 1.86 (m, 2H), 1.57 (m, 7H), 1.31 (m, 8H), 1.15 (m, 4H), 1.02 (m, 1H), 0.99 (s, 3H), 0.93 (d,  $J = 6.4$  Hz, 3H), 0.88 (d,  $J = 2.2$  Hz, 3H), 0.86 (d,  $J = 2.2$  Hz, 3H).  $^{13}\text{C NMR}$  (126 MHz,  $\text{CDCl}_3$ )  $\delta$  167.4, 156.6, 136.7, 135.2, 131.7, 128.6, 128.0, 127.8, 127.7, 127.5, 127.4, 127.1, 125.1, 120.4, 107.7, 72.1, 69.9, 56.5, 51.6, 41.9, 40.0, 39.4, 35.9, 35.4, 30.7, 29.7, 28.0, 27.1, 23.7, 22.8, 22.8, 22.5, 18.6, 18.1, 13.5. DART-HRMS:  $m/z$  calcd for  $\text{C}_{30}\text{H}_{46}\text{O}_3\text{NH}_4$   $[\text{MNH}_4]^+$ , 544.3791; found, 544.3792.

**6-Benzyloxy-2-naphthyl-VD3 Ester (54).**  $^1\text{H NMR}$  (500 MHz,  $\text{CDCl}_3$ )  $\delta$  8.53 (m, 1H), 8.04 (m, 1H), 7.86 (m, 1H), 7.75 (m, 1H), 7.49 (m, 2H), 7.42 (m, 2H), 7.35 (m, 1H), 7.28 (m, 1H), 7.25 (m, 1H), 5.46 (m, 1H), 5.21 (s, 2H), 2.10 (m, 1H), 2.04 (m, 1H), 1.86 (m, 2H), 1.54 (m, 6H), 1.42 (m, 1H), 1.35 (m, 2H), 1.25 (m, 3H), 1.15 (m, 3H), 1.11 (s, 3H), 1.03 (m, 1H), 0.95 (d,  $J = 6.5$  Hz, 3H), 0.88 (d,

$J = 1.9$  Hz, 3H), 0.87 (d,  $J = 1.9$  Hz, 3H).  $^{13}\text{C}$  NMR (126 MHz,  $\text{CDCl}_3$ )  $\delta$  166.7, 158.5, 136.9, 136.4, 131.0, 130.7, 128.6, 128.1, 128.0, 127.5, 126.8, 126.1, 126.0, 119.8, 106.9, 72.2, 70.1, 56.5, 51.7, 41.9, 40.0, 39.4, 35.9, 35.4, 30.6, 28.0, 27.1, 23.7, 22.8, 22.7, 22.5, 18.6, 18.1, 13.6. DART-HRMS:  $m/z$  calcd for  $\text{C}_{36}\text{H}_{46}\text{O}_3$   $[\text{M}]^+$ , 526.3447; found, 526.3453.

**3,5-Bis(benzyloxy)-VD3 Ester (59).**  $^1\text{H}$  NMR (500 MHz,  $\text{CDCl}_3$ )  $\delta$  7.45 (m, 4H), 7.40 (m, 4H), 7.35 (m, 2H), 7.33 (m, 2H), 6.83 (m, 1H), 5.39 (m, 1H), 5.09 (s, 4H), 2.08 (m, 1H), 1.99 (m, 1H), 1.82 (m, 2H), 1.54 (m, 5H), 1.40 (m, 5H), 1.26 (m, 3H), 1.15 (m, 4H), 1.03 (s, 3H), 0.95 (d,  $J = 6.4$  Hz, 3H), 0.90 (d,  $J = 2.3$  Hz, 3H), 0.89 (d,  $J = 2.2$  Hz, 3H).  $^{13}\text{C}$  NMR (126 MHz  $\text{CDCl}_3$ )  $\delta$  166.0, 159.7, 136.4, 132.8, 128.5, 128.0, 127.4, 108.2, 107.1, 70.2, 56.4, 51.5, 41.9, 39.8, 39.4, 35.9, 35.4, 30.4, 27.9, 27.0, 23.7, 22.7, 22.6, 22.5, 18.5, 18.0, 13.5. DART-HRMS:  $m/z$  calcd for  $\text{C}_{39}\text{H}_{51}\text{O}_4$   $[\text{MH}]^+$ , 583.3787; found, 583.3760.

**3,4,5-Tris(benzyloxy)-VD3 Ester (60).**  $^1\text{H}$  NMR (500 MHz,  $\text{CDCl}_3$ )  $\delta$  7.43 (m, 5H), 7.39 (m, 6H), 7.34 (m, 2H), 7.28 (m, 2H), 5.34 (m, 1H), 5.15 (m, 6H), 2.07 (m, 1H), 1.97 (m, 1H), 1.85 (m, 1H), 1.73 (m, 1H), 1.52 (m, 5H), 1.38 (m, 4H), 1.26 (m, 3H), 1.16 (m, 4H), 1.04 (m, 1H), 0.98 (s, 3H), 0.95 (d,  $J = 6.4$  Hz, 3H), 0.90 (d,  $J = 2.1$  Hz, 3H), 0.89 (d,  $J = 2.1$  Hz, 3H).  $^{13}\text{C}$  NMR (126 MHz,  $\text{CDCl}_3$ )  $\delta$  165.9, 152.4, 142.0, 137.4, 136.6, 128.5, 128.5, 128.1, 127.9, 127.9, 127.3, 125.9, 108.9, 77.2, 75.1, 72.3, 71.0, 56.4, 51.5, 41.9, 39.8, 39.4, 35.9, 35.4, 30.4, 28.0, 27.0, 23.7, 22.8, 22.5, 22.5, 18.5, 17.9, 13.4. DART-HRMS:  $m/z$  calcd for  $\text{C}_{46}\text{H}_{57}\text{O}_5$   $[\text{MH}]^+$ , 689.4206; found, 689.4202.

**2-Benzyloxy-3-pyridyl-VD3 Ester (61).**  $^1\text{H}$  NMR (500 MHz,  $\text{CDCl}_3$ )  $\delta$  8.13 (m, 1H), 7.82 (m, 1H), 7.35 (m, 5H), 6.57 (m, 1H), 5.28 (m, 1H), 5.15 (m, 2H), 2.02 (m, 1H), 1.90 (m, 1H), 1.83 (m, 1H), 1.65 (m, 1H), 1.49 (m, 6H), 1.22 (m, 10H), 1.01 (m, 1H), 0.92 (d,  $J = 6.5$  Hz, 3H), 0.88 (d,  $J = 2.1$  Hz, 3H), 0.86 (d,  $J = 2.0$  Hz, 3H), 0.84 (s, 3H).  $^{13}\text{C}$  NMR (126 MHz,  $\text{CDCl}_3$ )  $\delta$  164.0, 162.4, 142.2, 138.4, 135.3, 129.0, 128.6, 128.4, 119.8, 110.5, 72.5, 56.3, 52.5, 51.3, 41.8, 39.6, 39.4, 35.8, 35.3, 30.4, 27.9, 26.9, 23.7, 22.7, 22.5, 18.5, 17.8, 13.4. DART-HRMS:  $m/z$  calcd for  $\text{C}_{31}\text{H}_{44}\text{NO}_3$   $[\text{MH}]^+$ , 478.3321; found, 478.3329.

**2-Pyridyl-3-benzyloxy-VD3 Ester (62).**  $^1\text{H}$  NMR (500 MHz,  $\text{CDCl}_3$ )  $\delta$  7.74 (m, 1H), 7.69 (m, 1H), 7.51 (m, 2H), 7.39 (m, 2H), 7.33 (m, 1H), 6.97 (m, 1H), 5.48 (m, 3H), 2.06 (m, 2H), 1.85 (m, 2H), 1.54 (m, 6H), 1.38 (m, 4H), 1.26 (m, 2H), 1.15 (m, 3H), 1.12 (s, 3H), 1.02 (m, 1H), 0.95 (d,  $J = 6.5$  Hz, 3H), 0.89 (d,  $J = 2.1$  Hz, 3H), 0.88 (d,  $J = 2.0$  Hz, 3H).  $^{13}\text{C}$  NMR (126 MHz,  $\text{CDCl}_3$ )  $\delta$  164.9, 163.1, 145.9, 138.9, 137.0, 128.3, 128.2, 127.8, 118.4, 115.1, 72.7, 67.7, 56.4, 51.5, 41.9, 40.0, 39.4, 35.8, 35.3, 30.5, 27.9, 27.0, 23.7, 22.7, 22.6, 22.5, 18.5, 18.0, 13.3. DART-HRMS:  $m/z$  calcd for  $\text{C}_{31}\text{H}_{44}\text{NO}_3\text{NH}_4$   $[\text{MNH}_4]^+$ , 478.3321; found, 478.3350.

**General Procedure for Benzyl Deprotection.** To a solution of benzyl-protected ester (0.15 mmol) in MeOH:THF (2:1, 6 mL) was added palladium hydroxide (10% on carbon; 10 mg). The mixture was sealed with a rubber septum, sequentially purged with argon and hydrogen, and stirred under positive hydrogen pressure (1 atm) at RT for 12–18 h. The mixture was filtered through a Celite pad, rinsed with EtOAc (10 mL), and concentrated. The crude residue was purified using column chromatography ( $\text{SiO}_2$ , 10–40% EtOAc in hexanes) to yield final VD3 analogues in good yields (60–85%).

**3-Hydroxy-VD3 Ester (5).** Previously characterized.<sup>16</sup> HPLC: >98%,  $R_t = 7.4$  min (method A).

**2-Hydroxy-VD3 Ester (41).** HPLC: 95%,  $R_t = 14.5$  min (method B).  $^1\text{H}$  NMR (500 MHz,  $\text{CDCl}_3$ )  $\delta$  11.0 (s, 1H), 7.88 (m, 1H), 7.48 (m, 1H), 7.01 (m, 1H), 6.91 (m, 1H), 5.46 (m, 1H), 2.12 (m, 1H), 2.04 (m, 1H), 1.86 (m, 2H), 1.57 (m, 5H), 1.45 (m, 3H), 1.36 (m, 2H), 1.28 (m, 3H), 1.17 (m, 4H), 1.06 (s, 3H), 0.96 (d,  $J = 6.8$  Hz, 3H), 0.89 (d,  $J = 6.2$  Hz, 6H).  $^{13}\text{C}$  NMR (126 MHz  $\text{CDCl}_3$ )  $\delta$  170.2, 161.8, 135.4, 129.7, 119.1, 117.6, 113.0, 73.1, 56.4, 51.5, 41.9, 39.8, 39.4, 35.9, 35.4, 30.4, 28.0, 27.0, 23.7, 22.8, 22.6, 22.5, 18.6, 17.9, 13.5. IR (film)  $\nu_{\text{max}}$  3184, 3146, 3017, 2950, 2931, 2867, 1671, 1613, 1584, 1485, 1466, 1374, 1346, 1325, 1301, 1250, 1208, 1137, 1088, 1061, 1032, 937, 917, 883, 800, 755, 702, 666. DART-HRMS:  $m/z$  calcd for  $\text{C}_{25}\text{H}_{37}\text{O}_3$   $[\text{M} - \text{H}]^+$ , 385.2743; found, 385.2736.

**4-Hydroxy-VD3 Ester (42).** HPLC: 95%,  $R_t = 7.7$  min (method A).  $^1\text{H}$  NMR (500 MHz,  $\text{CDCl}_3$ )  $\delta$  7.96 (m, 2H), 6.87 (m, 2H), 5.80 (br s, 1H), 5.37 (m, 1H), 2.07 (m, 1H), 1.98 (m, 1H), 1.81 (m, 2H), 1.51 (m, 5H), 1.34 (m, 3H), 1.23 (m, 3H), 1.12 (m, 4H), 1.03 (s, 3H), 0.93 (d,  $J = 6.4$  Hz, 3H), 0.87 (dd,  $J = 6.6, 2.0$  Hz, 6H).  $^{13}\text{C}$  NMR (126 MHz  $\text{CDCl}_3$ )  $\delta$  166.5, 159.7, 131.8, 123.4, 115.2, 72.1, 56.4, 51.6, 41.9, 39.9, 39.4, 35.9, 35.4, 30.6, 28.0, 27.1, 23.7, 22.8, 22.6, 22.5, 18.6, 18.0, 13.5. IR (film)  $\nu_{\text{max}}$  3329 (br s), 3018, 2949, 2937, 2931, 2868, 1679, 1608, 1592, 1514, 1466, 1443, 1383, 1367, 1311, 1276, 1216, 1164, 1160, 1122, 1100, 1062, 938, 851, 754, 700, 668. DART-HRMS:  $m/z$  calcd for  $\text{C}_{25}\text{H}_{37}\text{O}_3\text{NH}_4$   $[\text{MNH}_4]^+$ , 404.3165; found, 404.3170.

**6-Hydroxy-1-naphthyl-VD3 Ester (55).** HPLC: 99%,  $R_t = 8.5$  min (method B).  $^1\text{H}$  NMR (500 MHz,  $\text{CDCl}_3$ )  $\delta$  8.90 (m, 1H), 8.04 (m, 1H), 7.82 (m, 1H), 7.45 (m, 1H), 7.23 (m, 2H), 6.04 (br s, 1H), 5.55 (m, 1H), 2.10 (m, 2H), 1.87 (m, 2H), 1.58 (m, 6H), 1.38 (m, 3H), 1.28 (m, 3H), 1.16 (m, 4H), 1.04 (m, 1H), 1.02 (s, 3H), 0.96 (d,  $J = 6.5$  Hz, 3H), 0.91 (d,  $J = 2.0$  Hz, 3H), 0.89 (d,  $J = 2.1$  Hz, 3H).  $^{13}\text{C}$  NMR (126 MHz,  $\text{CDCl}_3$ )  $\delta$  167.8, 153.6, 135.3, 131.5, 127.8, 127.8, 127.4, 126.6, 125.1, 119.4, 110.0, 72.4, 56.4, 51.6, 41.9, 39.9, 39.4, 35.9, 35.3, 30.6, 27.9, 27.1, 23.7, 22.8, 22.7, 22.5, 18.6, 18.1, 13.4. IR (film)  $\nu_{\text{max}}$  3400, 2953, 2929, 2917, 2896, 2865, 1706, 1684, 1624, 1597, 1516, 1465, 1374, 1263, 1233, 1217, 1196, 1133, 1063, 1007, 937, 834, 755, 720, 659. DART-HRMS:  $m/z$  calcd for  $\text{C}_{29}\text{H}_{40}\text{O}_3\text{NH}_4$   $[\text{MNH}_4]^+$ , 454.3321; found, 454.3347.

**6-Hydroxy-2-naphthyl-VD3 Ester (56).** HPLC: 96%,  $R_t = 8.8$  min (method B).  $^1\text{H}$  NMR (500 MHz,  $\text{CDCl}_3$ )  $\delta$  8.54 (m, 1H), 8.03 (m, 1H), 7.86 (m, 1H), 7.70 (m, 1H), 7.19 (m, 2H), 5.81 (br s, 1H), 5.48 (m, 1H), 2.10 (m, 1H), 2.05 (m, 1H), 1.86 (m, 2H), 1.55 (m, 6H), 1.42 (m, 1H), 1.36 (m, 2H), 1.27 (m, 3H), 1.15 (m, 3H), 1.11 (s, 3H), 1.02 (m, 1H), 0.95 (d,  $J = 6.5$  Hz, 3H), 0.88 (d,  $J = 1.9$  Hz, 3H), 0.87 (d,  $J = 1.9$  Hz, 3H).  $^{13}\text{C}$  NMR (126 MHz,  $\text{CDCl}_3$ )  $\delta$  167.0, 155.6, 137.0, 131.4, 131.0, 127.8, 126.4, 126.0, 125.8, 118.6, 109.4, 77.2, 72.4, 56.4, 51.6, 41.9, 39.9, 39.4, 35.9, 35.4, 30.6, 28.0, 27.1, 23.7, 22.8, 22.7, 22.5, 18.6, 18.1, 13.6. IR (film)  $\nu_{\text{max}}$  3379, 2946, 2920, 2914, 2902, 2869, 1685, 1680, 1624, 1480, 1436, 1394, 1365, 1288, 1276, 1200, 1158, 1096, 943, 865, 758, 753, 668, 473. DART-HRMS:  $m/z$  calcd for  $\text{C}_{29}\text{H}_{40}\text{O}_3$   $[\text{M}]^+$ , 436.2977; found, 436.2972.

**2-Indyl-VD3 Ester (58).** Analogue 58 was prepared according to the alternate method listed for analogue 40. HPLC: 98%,  $R_t = 46.9$  min (method D).  $^1\text{H}$  NMR (500 MHz,  $\text{CDCl}_3$ )  $\delta$  8.95 (br s, 1H), 7.69 (m, 1H), 7.42 (m, 1H), 7.32 (m, 1H), 7.19 (m, 1H), 7.15 (m, 1H), 5.43 (m, 1H), 2.09 (m, 1H), 2.02 (m, 1H), 1.86 (m, 2H), 1.55 (m, 6H), 1.43 (m, 2H), 1.35 (m, 2H), 1.15 (m, 4H), 1.09 (s, 3H), 1.02 (m, 1H), 0.95 (d,  $J = 6.5$  Hz, 3H), 0.88 (d,  $J = 1.9$  Hz, 3H), 0.87 (d,  $J = 1.8$  Hz, 3H).  $^{13}\text{C}$  NMR (126 MHz,  $\text{CDCl}_3$ )  $\delta$  161.9, 136.7, 127.9, 127.5, 125.2, 122.5, 120.7, 111.8, 108.2, 72.5, 56.5, 51.6, 42.0, 39.9, 39.4, 35.9, 35.4, 30.6, 29.7, 28.0, 27.0, 23.7, 22.8, 22.6, 22.5, 18.6, 18.0, 13.4. IR (film)  $\nu_{\text{max}}$  3480, 3436, 3323, 2953, 2932, 2919, 2867, 2854, 2848, 1683, 1528, 1466, 1457, 1395, 1382, 1341, 1309, 1251, 1208, 1158, 1147, 1062, 985, 937, 817, 774, 751, 737. DART-HRMS:  $m/z$  calcd for  $\text{C}_{27}\text{H}_{42}\text{NO}_2$   $[\text{MH}]^+$ , 410.3059; found, 410.3088.

**3,5-Bis(hydroxy)-VD3 Ester (63).** HPLC: >98%,  $R_t = 16.6$  min (method C).  $^1\text{H}$  NMR (500 MHz,  $\text{CDCl}_3$ )  $\delta$  7.14 (m, 2H), 6.58 (s, 1H), 5.57 (br s, 2H), 5.37 (m, 1H), 2.04 (m, 1H), 1.96 (m, 1H), 1.79 (m, 2H), 1.69 (m, 1H), 1.50 (m, 5H), 1.40 (m, 2H), 1.33 (m, 3H), 1.22 (m, 4H), 1.10 (m, 4H), 1.00 (s, 3H), 0.92 (d,  $J = 6.4$  Hz, 3H), 0.86 (d,  $J = 6.8$  Hz, 6H).  $^{13}\text{C}$  NMR (126 MHz,  $\text{CDCl}_3$ )  $\delta$  166.0, 156.8, 133.1, 109.1, 107.2, 72.8, 56.4, 51.5, 41.9, 39.8, 39.4, 35.9, 35.4, 30.4, 28.0, 27.0, 23.7, 22.8, 22.6, 22.5, 18.6, 17.9, 13.6. IR (film)  $\nu_{\text{max}}$  3430, 3019, 2947, 2934, 2866, 2399, 1699, 1605, 1347, 1302, 1215, 780, 755, 669, 653, 627. DART-HRMS:  $m/z$  calcd for  $\text{C}_{25}\text{H}_{38}\text{O}_4$   $[\text{M}]^+$ , 402.2770; found, 402.2770.

**3,4,5-Tris(Hydroxy)-VD3 Ester (64).** Analogue 64 was ultimately purified by using the following crystallization method: following two column chromatographic separations that afforded an impure oily mixture (30%), crude 64 was dissolved in diethyl ether inside a 1 dram vial. This was subsequently placed inside a 30 mL vial that was filled with 10 mL of pentanes. The cap was placed on the outer vial, parafilm, and covered with aluminum foil. After 3 days, pure white crystalline compound had formed within the inner vial, which was

filtered and repeatedly washed with pentanes. HPLC: >98%,  $R_t = 9.5$  min (method D).  $^1\text{H}$  NMR (500 MHz,  $\text{MeOD}:\text{CDCl}_3$ )  $\delta$  7.35 (s, 2H), 5.53 (m, 1H), 3.61 (s, 1H), 2.30 (m, 1H), 2.16 (m, 1H), 2.06 (m, 2H), 1.75 (m, 5H), 1.65 (m, 2H), 1.57 (m, 2H), 1.48 (m, 2H), 1.36 (m, 4H), 1.28 (s, 3H), 1.23 (m, 1H), 1.17 (d,  $J = 6.4$  Hz, 3H), 1.10 (d,  $J = 2.0$  Hz, 3H), 1.09 (d,  $J = 2.0$  Hz, 3H).  $^{13}\text{C}$  NMR (126 MHz,  $\text{MeOD}:\text{CDCl}_3$ )  $\delta$  166.9, 144.3, 137.5, 120.6, 108.6, 71.6, 55.9, 51.1, 41.3, 39.4, 38.9, 35.3, 34.8, 29.9, 27.3, 26.4, 23.1, 22.0, 21.8, 21.6, 17.8, 17.3, 12.7. IR (film)  $\nu_{\text{max}}$  3456, 3020, 2969, 2952, 2869, 1653, 1617, 1458, 1443, 1214, 1158, 1034, 768, 754, 749, 669. DART-HRMS:  $m/z$  calcd for  $\text{C}_{25}\text{H}_{37}\text{O}_4$   $[\text{M} - \text{H}]^+$ , 417.2641; found, 417.2648.

**2-Hydroxy-3-pyridyl-VD3 Ester (65).** HPLC: 97%,  $R_t = 15.8$  min (method D).  $^1\text{H}$  NMR (500 MHz,  $\text{CDCl}_3$ )  $\delta$  12.92 (br s, 1H), 8.16 (m, 1H), 8.02 (m, 1H), 6.59 (m, 1H), 5.35 (m, 1H), 2.05 (m, 1H), 1.94 (m, 1H), 1.84 (m, 1H), 1.69 (m, 2H), 1.52 (m, 5H), 1.35 (m, 5H), 1.23 (m, 5H), 1.14 (m, 4H), 1.00 (m, 1H), 0.95 (s, 3H), 0.92 (d,  $J = 6.5$  Hz, 3H), 0.87 (d,  $J = 2.0$  Hz, 3H), 0.86 (d,  $J = 1.9$  Hz, 3H).  $^{13}\text{C}$  NMR (126 MHz,  $\text{CDCl}_3$ )  $\delta$  165.4, 163.9, 141.1, 139.3, 119.5, 111.7, 72.7, 56.3, 51.4, 41.8, 39.7, 39.4, 35.8, 35.3, 30.4, 29.6, 27.9, 27.0, 23.7, 22.8, 22.6, 22.5, 18.5, 17.9, 13.6. IR (film)  $\nu_{\text{max}}$  3503 (br, weak), 3205 (br, weak), 2962, 2940, 2908, 2872, 2862, 2854, 1719, 1708, 1648, 1637, 1560, 1459, 1430, 1387, 1336, 1295, 1266, 1246, 1213, 1157, 1063, 1011, 979, 876, 757, 751, 725. DART-HRMS:  $m/z$  calcd for  $\text{C}_{24}\text{H}_{38}\text{NO}_3$   $[\text{MH}]^+$ , 388.2852; found, 388.2856.

**2-Pyridyl-3-hydroxy-VD3 Ester (66).** HPLC: >98%,  $R_t = 16.2$  min (method D).  $^1\text{H}$  NMR (500 MHz,  $\text{CDCl}_3$ )  $\delta$  10.3 (br s, 1H), 7.44 (m, 1H), 6.91 (m, 1H), 6.80 (m, 1H), 5.39 (m, 1H), 2.05 (m, 1H), 1.96 (m, 1H), 1.84 (m, 1H), 1.72 (m, 1H), 1.52 (m, 5H), 1.34 (m, 4H), 1.22 (m, 3H), 1.11 (m, 4H), 0.99 (m, 1H), 0.96 (s, 3H), 0.91 (d,  $J = 6.5$  Hz, 3H), 0.86 (d,  $J = 2.0$  Hz, 3H), 0.84 (d,  $J = 2.0$  Hz, 3H).  $^{13}\text{C}$  NMR (126 MHz,  $\text{CDCl}_3$ )  $\delta$  162.9, 160.9, 139.7, 134.1, 126.8, 108.9, 74.7, 56.1, 51.1, 41.7, 39.4, 39.3, 35.7, 35.2, 30.1, 27.9, 26.8, 23.6, 22.7, 22.5, 22.4, 18.4, 17.7, 13.3. IR (film)  $\nu_{\text{max}}$  3360 (br, w), 3017, 2952, 2933, 2891, 2869, 2855, 1723, 1657, 1611, 1467, 1296, 1277, 1260, 1215, 1158, 1139, 1060, 1001, 915, 819, 767, 753, 668. DART-HRMS:  $m/z$  calcd for  $\text{C}_{24}\text{H}_{38}\text{NO}_3\text{NH}_4$   $[\text{MNH}_4]^+$ , 388.2852; found, 388.2854.

**4-Amino-VD3 Ester (43).** To 39 (58 mg, 0.15 mmol) in DCM (2 mL) was added trifluoroacetic acid (1 mL), and the solution stirred for 16 h. The solution was diluted with saturated sodium bicarbonate (20 mL) and the aqueous layer washed with DCM (2  $\times$  30 mL). The combined organic fractions were dried ( $\text{Na}_2\text{SO}_4$ ), filtered, and concentrated. The crude residue was purified using column chromatography ( $\text{SiO}_2$ , 30–60% EtOAc in hexanes) to afford 43 as a clear oil in modest yield (65%). HPLC: 97%,  $R_t = 18.5$  min (method D).  $^1\text{H}$  NMR (500 MHz,  $\text{CDCl}_3$ )  $\delta$  7.86 (d,  $J = 8.4$  Hz, 2H), 6.64 (d,  $J = 8.3$  Hz, 2H), 5.35 (m, 1H), 4.03 (bs, 2H), 2.05 (m, 1H), 1.95 (m, 1H), 1.81 (m, 2H), 1.51 (m, 6H), 1.36 (m, 4H), 1.23 (m, 3H), 1.12 (m, 4H), 1.03 (s, 3H), 0.93 (d,  $J = 6.5$  Hz, 3H), 0.87 (d,  $J = 2.0$  Hz, 3H), 0.86 (d,  $J = 2.0$  Hz, 3H).  $^{13}\text{C}$  NMR (126 MHz,  $\text{CDCl}_3$ )  $\delta$  166.5, 131.5, 120.6, 113.7, 71.4, 60.3, 56.5, 51.7, 41.9, 40.0, 39.4, 35.9, 35.4, 31.5, 30.6, 28.0, 27.1, 23.7, 22.8, 22.6, 22.5, 18.6, 18.1, 14.1, 13.5. IR (film)  $\nu_{\text{max}}$  3451 (br, s), 3018, 2952, 2868, 1683, 1622, 1272, 1215, 1172, 1113, 851, 769, 749, 668. DART-HRMS: calcd for  $\text{C}_{25}\text{H}_{39}\text{NO}_2$   $[\text{M}]^+$ , 385.2981; found, 385.2968.

**Biological Assay Protocols. General Information.** Protocols for general cell culture, qPCR (Hh pathway and VDR), and VDR binding assays are as previously described.<sup>15,16</sup>  $20\alpha$ -Hydroxycholesterol and  $22(\text{S})$ -hydroxycholesterol (OHCs) were purchased from Sigma-Aldrich. VD3 for biological studies was purchased from Sigma-Aldrich. Data was analyzed using GraphPad Prism 5, and reported values represent mean  $\pm$  SEM for at least two separate experiments performed in triplicate.

**Fluorescence Binding Assays.**<sup>30–33</sup> For flow cytometry experiments, HEK293T cells were seeded in 10 cm cell culture dishes ( $2.5 \times 10^6$  cells) and incubated overnight (37  $^\circ\text{C}$ , 5%  $\text{CO}_2$ ). Cells were transfected with Smo-Myc<sub>3</sub> expression plasmid<sup>30</sup> (24  $\mu\text{g}$ ) using Lipofectamine 2000 reagent (60  $\mu\text{L}$ ) was added and the cells returned to the incubator overnight. The next day, cells were split into a single 6-well plate and incubated overnight. The next day (2 days post-transfection) cells were incubated in DMEM containing 10% FBS,

BODIPY-Cyc (5 nM), and various concentrations of Cyc, VD3, or 5 at 37  $^\circ\text{C}$  for 4 h. Cells were trypsinized, centrifuged, and resuspended in 500  $\mu\text{L}$  of phosphate buffered saline (PBS) for flow cytometry analysis. To determine transfection efficiency, cells were fixed with 2% PFA (15 min), permeabilized with 90% ethanol (30 min, 4  $^\circ\text{C}$ ), and blocked for nonspecific binding with 10% FBS in PBS (15 min, RT). Cells were incubated with anti-Myc antibody (1:800, Cell Signaling Technology) for 1 h at RT, followed by Alexa Flour-647 donkey anti-rabbit antibody (1:1000, Invitrogen) for 30 min at RT. Finally, cells were analyzed for green fluorescence using flow cytometry.

For isolated membrane experiments, HEK293T cells were seeded and transfected as described above. Cells were collected 24 h post-transfection and washed with PBS (2 $\times$ ) and water (1 $\times$ ). Cells were resuspended in hypotonic buffer (50 mM Tris-HCl, 1 mM EDTA, pH 7.5, protease inhibitor cocktail) and incubated at 4  $^\circ\text{C}$  for 10 min. Cells were permeabilized by repeatedly passing them through a syringe (25 times, 26 gauge). Cells were centrifuged (500g, 10 min) to pellet the larger cellular components. The supernatant was removed and recentrifuged (20000g, 30 min) to isolate the membranes incorporating the full-length Smo. The pellet was resuspended in hypotonic buffer and stored ( $-80$   $^\circ\text{C}$ ). For the fluorescence polarization assay, processed Smo-transfected membranes (10  $\mu\text{g}$ /well) were incubated with BODIPY-Cyc (5 nM) and various concentrations of Cyc, VD3, or 5 in hypotonic buffer (total volume of 100  $\mu\text{L}$ ) in a 96-well black-sided, flat bottom plate (Costar). Membranes were incubated at 30  $^\circ\text{C}$  for 5 h before FP was analyzed on a Synergy H1 hybrid multi-mode microplate reader (excitation 485 nM, emission 528 nM).

**VDRi Assay.** C3H10T1/2 cells were seeded into 24-well tissue culture treated plates 24 h prior to transfection. Lipofectamine 2000 (2.1  $\mu\text{L}$ , Invitrogen) was mixed with mouse VDR-specific siRNA (2.5  $\mu\text{L}$  of a 20  $\mu\text{M}$  stock solution, Dharmacon) in OptimEM reduced serum media (95.4  $\mu\text{L}$ , Life Technologies). Transfection solution (100  $\mu\text{L}$ /well) was added dropwise to cells supplemented with BME (400  $\mu\text{L}$ /well) containing 0.5% fetal bovine serum (Atlanta Biologicals) and 1% penicillin/streptomycin/L-glutamine (Cellgro) and plates returned to the incubator (37  $^\circ\text{C}$ , 5%  $\text{CO}_2$ ). Following a 6 h incubation period, transfection media was replaced with complete growth media and cells incubated overnight. Cells were treated with VD3 (5  $\mu\text{M}$ ), calcitriol (0.5  $\mu\text{M}$ ), 5 (5  $\mu\text{M}$ ), or control 24 h post-transfection. RNA isolation and cDNA synthesis was performed 24 h post-treatment (48 h post-transfection) using the Cells-to-Ct kit (Ambion) following the manufacturer's protocol and qPCR analysis of target genes followed standard procedures.<sup>15,16</sup>

## ■ ASSOCIATED CONTENT

### ● Supporting Information

$^1\text{H}$  and  $^{13}\text{C}$  NMR spectra for all new intermediates and final VD3 analogues. This material is available free of charge via the Internet at <http://pubs.acs.org>.

## ■ AUTHOR INFORMATION

### Corresponding Author

\*Phone: 1-806-486-8446. Fax: 1-860-486-6857. E-mail: kyle.hadden@uconn.edu.

### Author Contributions

The manuscript was written through contributions of all authors. All authors have given approval to the final version of the manuscript.

### Notes

The authors declare no competing financial interest.

## ■ ACKNOWLEDGMENTS

We gratefully acknowledge support of this work by the V Foundation for Cancer Research (V Scholar, M.K.H.), the Charles H. Hood Foundation, the University of Connecticut Research Foundation, and the American Cancer Society (RSG-

13-131-01). Daniel Madden, Daniel DeCarlo, and Steven M. Lemieux recognize the University of Connecticut for Undergraduate Research support. ASZ001 cells were provided by Dr. Ervin Epstein (Children's Hospital Oakland Research Institute). The Smo-Myc<sub>3</sub> expression plasmid was a kind gift from James Chen (Stanford University).

## ABBREVIATIONS USED

Hh: Hedgehog; Gli: glioblastoma associated oncogene; Ptch: patched; Cyp24a1: 1,25-dihydroxyvitamin D<sub>3</sub> 24-hydroxylase; VD<sub>3</sub>: vitamin D<sub>3</sub>; VDR: vitamin D receptor

## REFERENCES

- (1) Yang, L.; Xie, G.; Fan, Q.; Xie, J. Activation of the hedgehog signaling pathway in human cancer and the clinical implications. *Oncogene* **2010**, *29*, 469–481.
- (2) Epstein, E. H. Basal cell carcinomas: attack of the hedgehog. *Nature Rev. Cancer* **2008**, *8*, 743–754.
- (3) Berman, D. M.; Karhadkar, S. S.; Hallahan, A. R.; Pritchard, J. I.; Eberhart, C. G.; Watkins, D. N.; Chen, J. K.; Cooper, M. K.; Taipale, J.; Olson, J. M.; Beachy, P. A. Medulloblastoma growth inhibition by hedgehog pathway blockade. *Science* **2002**, *297*, 1559–1561.
- (4) Ling, G.; Ahmadian, A.; Persson, A.; Unden, A. B.; Afink, G.; Williams, C.; Uhlen, M.; Toftgard, R.; Lundeberg, J.; Ponten, F. PATCHED and p53 gene alterations in sporadic and hereditary basal cell cancer. *Oncogene* **2001**, *20*, 7770–7778.
- (5) Reifemberger, J.; Wolter, M.; Knobbe, C. B.; Kohler, B.; Schonicke, A.; Scharwachter, C.; Kumar, K.; Blaschke, B.; Ruzicka, T.; Reifemberger, G. Somatic mutations in the PTCH, SMOH, SUFUH, and TP53 genes in sporadic basal cell carcinomas. *Br. J. Dermatol.* **2005**, *152*, 43–51.
- (6) Klesse, L. J.; Bowers, D. C. Childhood medulloblastoma: current status of biology and treatment. *CNS Drugs* **2010**, *24*, 285–301.
- (7) Peukert, S.; Miller-Moslin, K. Small-molecule inhibitors of the hedgehog signaling pathway as cancer therapeutics. *ChemMedChem* **2010**, *5*, 500–512.
- (8) Hadden, M. K. Hedgehog pathway inhibitors: a patent review (2009–present). *Expert Opin. Ther. Pat.* **2013**, *23*, 345–361.
- (9) Rudin, C. M.; Hann, C. L.; Lartera, J.; Yauch, R. L.; Callahan, C. A.; Fu, L.; Holcomb, T.; Stinson, J.; Gould, S. E.; Coleman, B.; LoRusso, P. M.; Von Hoff, D. D.; de Sauvage, F. J.; Low, J. A. Treatment of medulloblastoma with hedgehog pathway inhibitor GDC-0449. *N. Engl. J. Med.* **2009**, *361*, 1173–1178.
- (10) Dijkgraaf, G. J. P.; Aliche, B.; Weinmann, L.; Januario, T.; West, K.; Modrusan, Z.; Burdick, D.; Goldsmith, R.; Robarge, K.; Sutherland, D.; Scales, S. J.; Gould, S. E.; Yauch, R. L.; de Sauvage, F. J. Small molecule inhibition of GDC-0449 refractory smoothed mutants and downstream mechanisms of drug resistance. *Cancer Res.* **2011**, *71*, 435–444.
- (11) Chang, A. L. S.; Oro, A. E. Initial assessment of tumor regrowth after vismodegib in advanced basal cell carcinoma. *Arch. Dermatol.* **2012**, *148*, 1324–1325.
- (12) Tang, J. Y.; Mackay-Wiggan, J. M.; Aszterbaum, M.; Yauch, R. L.; Lindgren, J.; Chang, K.; Coppola, C.; Chanana, A. M.; Marji, J.; Bickers, D. R.; Epstein, E. H. Inhibiting the hedgehog pathway in patients with the basal-cell nevus syndrome. *N. Engl. J. Med.* **2012**, *366*, 2180–2188.
- (13) Banerjee, U.; Ghosh, M.; Hadden, M. K. Evaluation of vitamin D<sub>3</sub> A-ring analogues as hedgehog pathway inhibitors. *Bioorg. Med. Chem. Lett.* **2012**, *22*, 1330–1334.
- (14) Tang, J. Y.; Xiao, T. Z.; Oda, Y.; Chang, K. S.; Shpall, E.; Wu, A.; So, P.-L.; Hebert, J.; Bikle, D.; Epstein, E. H. Vitamin D<sub>3</sub> inhibits hedgehog signaling and proliferation in murine basal cell carcinomas. *Cancer Prev. Res.* **2011**, *4*, 744–751.
- (15) DeBerardinis, A. M.; Banerjee, U.; Miller, M.; Lemieux, S.; Hadden, M. K. Probing the structural requirements for vitamin D<sub>3</sub> inhibition of hedgehog signaling. *Bioorg. Med. Chem. Lett.* **2012**, *22*, 4859–4863.
- (16) DeBerardinis, A. M.; Banerjee, U.; Hadden, M. K. Identification of vitamin D<sub>3</sub>-based hedgehog pathway inhibitors that incorporate an aromatic A-ring isostere. *ACS Med. Chem. Lett.* **2013**, *4*, 590–595.
- (17) Bijlsma, M. F.; Spek, C. A.; Zivkovic, D.; van de Water, S.; Rezaee, F.; Peppelenbosch, M. P. Repression of smoothed by patched-dependent (pro-)vitamin D<sub>3</sub> secretion. *PLoS Biol.* **2006**, *4*, e232.
- (18) Somu, R. V.; Boshoff, H.; Qiao, C.; Bennett, E. M.; Barry, C. E.; Aldrich, C. C. Rationally designed nucleoside antibiotics that inhibit siderophore biosynthesis of *Mycobacterium tuberculosis*. *J. Med. Chem.* **2006**, *49*, 31–34.
- (19) Kuwano, R.; Kusano, H. Benzyl protection of phenols under neutral conditions: palladium-catalyzed benzylations of phenols. *Org. Lett.* **2008**, *10*, 1979–1982.
- (20) Nguyen, T.-T.-T.; Simon, F.-X.; Schmutz, M.; Mésini, P. J. Direct functionalization of self-assembled nanotubes overcomes unfavorable self-assembling processes. *Chem. Commun.* **2009**, 3457–3459.
- (21) Su, X.; Surry, D. S.; Spandl, R. J.; Spring, D. R. Total synthesis of sanguin H-5. *Org. Lett.* **2008**, *10*, 2593–2596.
- (22) Jullien, L.; Canceill, J.; Valeur, B.; Bardez, E.; Lefèvre, J.-P.; Lehn, J.-M.; Marchi-Artzner, V.; Pansu, R. Multichromophoric cyclodextrins. 4. Light conversion by antenna effect. *J. Am. Chem. Soc.* **1996**, *118*, 5432–5442.
- (23) Sieburth, S. M.; Hiel, G.; Lin, C.-H.; Kuan, D. P. Intramolecular [4 + 4] photocycloaddition of 2-pyridones tethered by a three-carbon chain: studies on the formation of cycloadducts and control of stereogenesis. 3. *J. Org. Chem.* **1994**, *59*, 80–87.
- (24) Mack, H.; Kling, A.; Jantos, K.; Moeller, A.; Hornberger, W.; Hutchins, C. Carboxamide Compounds and Their Use as Calpain Inhibitors. U.S. Patent 8,283,363, October 9, 2012.
- (25) Norman, M. H.; Rigdon, G. C.; Hall, W. R.; Navas, F., III. Structure–Activity Relationships of a Series of Substituted Benzamides: Potent D<sub>2</sub>/5-HT<sub>2</sub> Antagonists and 5-HT<sub>1A</sub> Agonists as Neuroleptic Agents. *J. Med. Chem.* **1996**, *39*, 1172–1188.
- (26) Majmudar, J. D.; Hodges-Loaiza, H. B.; Hahne, K.; Donelson, J. L.; Song, J.; Shrestha, L.; Harrison, M. L.; Hrycyna, C. A.; Gibbs, R. A. Amide-modified prenylcysteine based IcmT inhibitors: structure–activity relationships, kinetic analysis and cellular characterization. *Bioorg. Med. Chem.* **2012**, *20*, 283–295.
- (27) Huo, C.; Shi, G.; Lam, W. H.; Chen, D.; Cui, Q. C.; Duo, Q. P.; Chan, T. H. Semi-synthesis and proteasome inhibition of D-ring deoxy analogs of (–)-epigallocatechin gallate (EGCG), the active ingredient of green tea extract. *Can. J. Chem.* **2008**, *86*, 495–502.
- (28) Hawker, C. J.; Lee, R.; Frechet, J. M. J. One-step synthesis of hyperbranched dendritic polyesters. *J. Am. Chem. Soc.* **1991**, *113*, 4583–4588.
- (29) Thapa, M.; Kim, Y.; Desper, J.; Chang, K.-O.; Hua, D. H. Synthesis and antiviral activity of substituted quercetins. *Bioorg. Med. Chem. Lett.* **2012**, *22*, 353–356.
- (30) Chen, J. K.; Taipale, J.; Cooper, M. K.; Beachy, P. A. Inhibition of hedgehog signaling by direct binding of cyclopamine to smoothed. *Genes Dev.* **2002**, *16*, 2743–2748.
- (31) De Rivoire, M.; Ruel, L.; Varjosalo, M.; Loubat, A.; Bidet, M.; Théron, P.; Mus-Veteau, I. Human receptors patched and smoothed partially transduce hedgehog signal when expressed in *Drosophila* cells. *J. Biol. Chem.* **2006**, *281*, 28584–28595.
- (32) Rominger, C. M.; Bee, W. L.; Copeland, R. A.; Davenport, E. A.; Gilmartin, A.; gontarek, R.; Hornberger, K. R.; Kallal, L. A.; Lai, Z.; Lawrie, K.; Lu, Q.; McMillan, L.; Truong, M.; Tummino, P. J.; Turunen, B.; Will, M.; Zuercher, W. J.; Rominger, D. H. Evidence for allosteric interactions of antagonist binding to the smoothed receptor. *J. Pharmacol. Exp. Ther.* **2009**, *329*, 995–1005.
- (33) Allen, M.; Reeves, J.; Mellor, G. High-throughput fluorescence polarization: a homogenous alternative to radioligand binding for cell surface receptors. *J. Biomol. Screening* **2000**, *5*, 63–69.

(34) Kageyama, Y.-I.; Yamazaki, Y.; Afify, A. S.; Ogawa, Y.; Okada, T.; Okuno, H. Stereoselective hydrolysis of xenobiotic esters by different cell lines from rat liver and hepatoma and its application to chiral prodrugs for designated growth suppression of cancer cells. *Chirality* **1995**, *7*, 297–304.

(35) Tian, L.; Yang, Y.; Wysocki, L. M.; Arnold, A. C.; Hu, A.; Ravichandran, B.; Sternson, S. M.; Looger, L. L.; Lavis, L. D. Selective esterase-ester pair for targeting small molecules with cellular specificity. *Proc. Natl. Acad. Sci. U. S. A.* **2012**, *109*, 4756–4761.

(36) Aich, U.; Campbell, C. T.; Elmouelhi, N.; Weier, C. A.; Sampathkumar, S.-G.; Choi, S. S.; Yarema, K. J. Regioisomeric SCFA attachment to hexosamines separates metabolic flux from cytotoxicity and MUC1 suppression. *ACS Chem. Biol.* **2008**, *3*, 230–240.

(37) Lavis, L. D. Ester bonds in prodrugs. *ACS Chem. Biol.* **2008**, *3*, 203–206.

(38) Nedelcu, D.; Liu, J.; Xu, Y.; Jao, C.; Salic, A. Oxysterols binding to the extracellular domain of smoothed in hedgehog signaling. *Nature Chem. Biol.* **2013**, *9*, 557–564.

(39) Myers, B. R.; Sever, N.; Chonog, Y. C.; Kin, J.; Belani, J. D.; Rychnovsky, S.; Bazan, J. F.; Beachy, P. A. Hedgehog pathway modification by multiple lipid binding sites on the smoothed effector of signal response. *Dev. Cell* **2013**, *26*, 346–357.

(40) Nachtergaele, S.; Whalen, D. M.; Mydock, L. K.; Zhao, Z.; Malinauskas, T.; Krishnan, K.; Ingham, P. W.; Covey, D. F.; Siebold, C.; Rohatgi, R. Structure and function of the smoothed extracellular domain in vertebrate hedgehog signaling. *eLife* **2013**, *2*, e01340.

(41) Uhmann, A.; Niemann, H.; Lammering, B.; Henkel, C.; Heb, I.; Nitzki, F.; Fritsch, A.; Prüfer, N.; Rosenberger, A.; Dullin, C.; Schraepfer, A.; Reifenberger, J.; Schweyer, S.; Pietsch, T.; Strutz, F.; Schulz-Schaeffer, W.; Hahn, H. Antitumoral effects of calcitriol in basal cell carcinomas involve inhibition of hedgehog signaling and induction of vitamin D receptor signaling and differentiation. *Mol. Cancer Ther.* **2011**, *10*, 2179–2188.